Sulphonated polyisobutylene telechelic ionomers: 12. Solid-state mechanical properties

Shriram Bagrodia*, Martin R. Tant† and Garth L. Wilkes
Department of Chemical Engineering and Polymer Materials and Interfaces Laboratory, Virginia Polytechnic Institute and State University, Blacksburg, Virginia 24061-6496, USA

and Joseph P. Kennedy
Institute of Polymer Science, The University of Akron, Akron, Ohio 44325, USA

(Received 11 September 1986; revised 24 April 1987; accepted 3 June 1987)

The solid-state mechanical properties of well defined sulphonated polyisobutylene telechelic ionomers are presented. Specifically, the effect of (1) molecular architecture, (2) molecular weight, (3) type of cation used for neutralization and (4) excess neutralizing agent has been investigated. In addition, the effect of moisture and ionic plasticizer on the stress–strain behaviour has also been studied.

These ionomers do not display the characteristic small-angle X-ray scattering (SAXS) peak, which is indicative of the presence of clusters, above a number-average molecular weight of about 10000. However, below this molecular weight a weak shoulder is sometimes observed on the SAXS curve. The tri-arm species form a network structure at ambient temperatures which results in materials with good mechanical properties. The mechanical properties of the linear difunctional species are inferior to those of the three-arm star trifunctional species due to a less well developed network structure. The monofunctional species are very tacky at ambient temperatures and cannot be handled as solid materials. However, by their incorporation into the trifunctional systems they do serve as a model for 'dangling ends'. As expected, these blends display significantly different properties than those possessed with the pure trifunctional species.

Addition of excess neutralizing agent significantly increases the high deformation properties with little effect on Young's modulus. A simple morphological model has been postulated in which it is suggested that the excess neutralizing agent resides at the ionic sites rather than being uniformly distributed throughout the matrix. Zinc-neutralized ionomers show stress–strain behaviour which is comparable to the potassium- and calcium-neutralized materials at ambient conditions, but the softening temperature is lower for the zinc neutralized material. Water absorption in these materials is relatively low. Addition of zinc stearate, an ionic plasticizer, facilitates melt processing by lowering the viscosity at high temperatures yet at ambient temperatures it crystallizes and acts as a reinforcing filler thus increasing Young's modulus.

(Keywords: ionomers; telechelics; mechanical properties; thermoplastic elastomers; polyisobutylene)

INTRODUCTION

The utilization of ionic interactions in polymers has recently attracted widespread interest since it provides an additional means of controlling polymer structure and properties. One class of ion-containing polymers which is currently of great practical and theoretical interest in both the industrial and academic sectors is that of ionomers. An ionomer is a polymer which generally has less than 15 mol% ionic groups on an otherwise non-polar chain. (This has served as a working definition of the term *ionomer* for two decades. It should be noted, however, that equal mole percentages of ions in different polymers may result in different volume percentages due to variations in the molecular weight of the repeat units.) Neutralization of these ionic groups with ions of the opposite charge results in strong coulombic associations and thus the formation of an ionic network. As would be expected, the ionomer may display properties which are dramatically different from those of the parent polymer. In addition, materials with a broad spectrum of properties may be created by varying the ionic content, neutralizing cation, extent of neutralization, etc. Recent reviews of the structure and properties of ionomers have been published by MacKnight and Ernest[1], Banzuin and Eisenberg[2], Longworth[3] and Mauritz and Hopfinger[4].

Although much of the earlier work on ionomers focused on non-elastomeric materials, attention has more recently shifted to elastomeric ionomers due to their commercial potential as thermoplastic elastomers, i.e. elastomers which flow at high temperatures yet retain their network structure at ambient temperatures. For a material to function as a useful elastomer, the polymer molecules must, of course, be connected in some way to one another to form a three-dimensional network structure. Classically, the crosslinking of polymer molecules has been accomplished via permanent covalent crosslinks which, once formed, prevent flow. However, if an elastomer is crosslinked via strong ionic bonding

---

* Present address: Tennessee Eastman Company, Kingsport, TN 37662, USA
† Present address: Dow Chemical USA, Freeport, TX 77541, USA

0032–3861/87/132207–20$03.00

rather than permanent covalent bonding, the potential exists for a thermoplastic elastomer. The ionic bonds form physical crosslinks between the polymer molecules which promote good elastomeric character, but at higher temperatures these bonds become sufficiently labile to allow the material to flow and be processed as a thermoplastic elastomer.

In the conventional ionomers the ionic groups are distributed randomly along the polymer chain. The resulting network structure is thus less than well defined. Another approach is to prepare telechelic polymers which have the ionic groups located only at the chain ends. This defined chain microstructure leads to a network whose structure is much better defined than those resulting from the traditional ionomers in terms of molecular weight between ionic regions. The task of relating structure and properties is thus somewhat simplified. This approach has been taken in the present work to synthesize sulphonated polyisobutylene telechelic ionomers with a variety of molecular architectures. Specifically, three different chain microstructures have been prepared—linear monofunctional, linear difunctional and three-arm star trifunctional. In this paper we present the results of studies concerning the solid-state structure and mechanical properties of these materials. However, before beginning the discussion of this work, we will present a brief overview of previous work on elastomeric ionomers, in addition to some discussion of ionomers in general, in order to establish the fundamental structure–property behaviour of these materials.

PREVIOUS WORK ON ELASTOMERIC IONOMERS

The unique properties possessed by ionomers are, of course, a direct result of the interactions between ionic groups. Realizing the importance of understanding the structure of ionomers, Eisenberg first attempted to describe the nature of the ionic interactions and the resulting influence upon morphology[5]. He assumed that the basic structure present is the contact ion pair in which the cation and anion are separated by the sum of their ionic radii. The electrostatic attraction between ion pairs results in the formation of regions consisting only of ionic species. These ionic regions, termed multiplets, specifically exclude the hydrocarbon or non-ionic portions of the polymer chains. The size of a multiplet, *if a spherical structure is assumed*, is thus limited by steric considerations. Eisenberg suggested that multiplets may further associate to form larger structures called clusters. Cluster formation occurs at higher ion concentrations. The multiplets which make up the cluster are separated by a hydrocarbon skin consisting of the non-ionic portions of the polymer chains. The maximum cluster size is limited by the elasticity of the polymer molecules. Eisenberg and Navratil have suggested, based upon their extensive studies of the structure and properties of polystyrene ionomers, that a transition from multiplet to cluster morphology occurs above a critical concentration of ionic groups[6–9]. For example, in sulphonated polystyrene this critical ion content has been suggested to be about 6 mol% based on a combination of viscoelastic, dielectric and Raman spectroscopy data. In the viscoelasticity studies, time–temperature superposition for stress relaxation was found to hold below this ion concentration but fails at higher concentrations. In addition, a small-angle X-ray scattering (SAXS) peak was observed above this critical ion concentration but not for materials below this ion content, although Weiss and Lefelar[10] have recently observed the peak well below 6 mol%. This small-angle peak has come to represent evidence of a clustered morphology, and several morphological models have been based upon it. These have included the models of Longworth and Vaughan[11], Marx *et al.*[12], Binsbergen and Kroon[13], MacKnight *et al.*[14] and Graiver *et al.*[15] More recently, Yarusso and Cooper[16,17] have proposed a model which attributes the small-angle X-ray scattering peak to interparticle interference between small ionic domains arranged in the hydrocarbon matrix with a liquid-like degree of order. Such analytical techniques as EXAFS (extended X-ray absorption fine structure)[18–21], XANES (X-ray absorption near edge structure)[20], *FT*i.r. (Fourier transform infra-red) spectroscopy[22] and ESR (electron spin resonance) spectroscopy[23] have also been applied to probe the structure of the ionic aggregates. Recent theoretical efforts to describe the structure of ionomers have been due primarily to Forsman and coworkers[24,25] and Dreyfus[26,27]. Suffice it to say that there remains considerable controversy concerning the nature of ionic associations in ionomers, particularly with regard to the higher-order cluster structure.

Early in the development of elastomeric ionomers, carboxylic acid groups were introduced into the polymer chain as a means of controlling polarity. The first such commercial product was a butadiene–styrene–acrylic acid terpolymer latex (trade name Hycar 1571) marketed by B.F. Goodrich in 1949[28]. It was Brown who first neutralized carboxylated elastomers with metal oxides in the early 1950s, thus actually forming ionically crosslinked elastomers—the first ionomers[29]. Thus Brown was the pioneer whose work catalysed the development of an entire new class of polymer materials. In 1957 and 1963 he published reviews describing the carboxylated elastomers[28,30]. A more recent review of carboxylated elastomers through the early 1970s was presented by Jenkins and Duck[31].

Following the pioneering work of Brown, the field of ionomers grew rapidly. However, most of the research was focused on carboxylated polystyrene- and polyethylene-based ionomers, which are non-elastomeric in nature. This shift in emphasis to non-elastomeric ionomers was perhaps due to the poor ultimate mechanical properties of carboxylated elastomers. However, sulphonated elastomers were later found to have much better ultimate mechanical properties than the earlier carboxylated elastomers. Using polystyrene, Lundberg and Makowski[32] also demonstrated very clearly that the sulphonate materials show much stronger ionic association than the corresponding carboxylate materials.

With the advent of the sulphonated ionomers, new interest in the ion-containing elastomers was generated. Exxon patents in the mid-1970s[33–35] on sulphonated EPDM materials revitalized the efforts to probe the potential of elastomeric ionomers. However, it was not until 1978 that the first data on EPDM-based ionomers were published in the open literature. Since then there has been a large increase in research efforts aimed at developing an understanding of these and other elastomeric ionomers.

The EPDM systems are terpolymers of ethylene, propylene and a non-conjugated diene monomer (e.g. ethylidene norbornene or ENB) which are polymerized by a Ziegler–Natta or coordination mechanism. Details of the synthesis, sulphonation and neutralization procedures have been presented by Makowski and Lundberg and coworkers[36–43], who have extensively studied the mechanical behaviour as well as the melt and solution rheological behaviour of these ionomers. They note that the base EPDM polymer shows only a short pseudo-rubbery plateau near room temperature, indicating the presence of entanglements but no crosslinking. However, upon light sulphonation (0.6 mol%) and neutralization, a well defined rubbery plateau is observed. Dynamic mechanical measurements reveal only one major loss peak near the glass transition temperature (T_g), with no significant effect on T_g. The time–temperature superposition principle was found to be valid for these ionomers containing up to 1.6 mol% ionic content. These observations indirectly support a non-clustered or multiplet morphology in these EPDM sulphonate ionomers. The effect of different cations on the tensile and melt flow behaviour of these ionomers was also investigated by Makowski *et al.*[38] The cations studied were Li^+, Na^+, Mg^{2+}, Ca^{2+}, Ba^{2+}, Co^{2+}, Zn^{2+} and Pb^{2+}. Zinc-neutralized ionomers displayed the highest melt index (0.75 at 190°C, 478 psi) followed by lead (0.1), while the other materials did not flow at all (melt index of 0). The tensile properties of zinc-neutralized ionomers were found to be equal to or greater than those for the other materials. This combination of good mechanical properties at ambient temperatures and low melt viscosity at elevated temperatures indicate that the zinc-neutralized ionomers are the most suitable from a melt processing point of view.

These workers also found that the melt viscosity of zinc-neutralized EPDM sulphonate ionomers can be further reduced by use of an ionic plasticizer such as zinc stearate. The zinc stearate interacts strongly with the sulphonate groups at elevated temperatures, thereby tending to break up the ionic associations and reduce the viscosity. Upon cooling to ambient temperatures the zinc stearate separates via crystallization and acts as a reinforcing filler to enhance the modulus. Thus, through a suitable choice of molecular weight, sulphonate content, neutralizing cation and ionic plasticizer, it is possible to obtain metal sulphonate EPDMs with good mechanical properties and sufficiently low melt viscosity for processing.

Elastomeric ionomers based on polypentenamers have been studied by MacKnight and coworkers. Polypentenamers are very low T_g elastomers ($\sim -95°C$) resulting from the metal-carbene-catalysed ring-opening coordination polymerization of cyclopentene. This reaction results in a linear chain with a double bond in each repeat unit. Ionic groups such as thioglycolate[44], phosphonate[45,46] and sulphonate[47,48] were grafted onto this unsaturated elastomer to various levels and the properties of the resulting materials were compared. The study was primarily focused on calorimetric and dynamic mechanical behaviour. It was determined that the calorimetric T_g is affected differently by the different cations, the effect increasing in the order thioglycolate $\simeq$ carboxylate < sulphonate < phosphonate. The dynamic mechanical behaviour suggests that a separate ionic phase (clustering) exists which acts as a reinforcing filler in addition to the expected ionic crosslinking effect. The dynamic mechanical data also suggest that clustering apparently does not occur in the phosphonate ionomers at any of the ion concentrations studied, but occurs above 10 mol% ion content in the sulphonate ionomers. Thioglycolate and carboxylate ionomer samples all had ion concentrations of less than 10 mol% and did not display evidence of clustering.

A fourth class of elastomeric ionomer system that has been studied is based on segmented polyurethanes. These polyurethanes typically consist of chemical units which are rigid at ambient temperatures alternating with soft, flexible units. The hard segment typically consists of an aromatic diisocyanate linked by short diol or diamine chain extenders. The soft segment is normally a polyester or polyether. In the solid state the two types of segments may be phase-segregated into microdomains which can be either amorphous or semicrystalline. The hard domains act as thermally reversible multifunctional crosslink points as well as a reinforcing filler. The incorporation of ionic groups into the hard segment was found to have a strong effect on the properties of polyurethanes in bulk and solution by Dieterich *et al.*[49] Based on the variety of interactions possible and the ability to swell or dissolve the materials in an aqueous environment, these workers suggested a wide range of potential uses including latex paints or coatings, adhesives and microporous sheeting materials.

More recently, Cooper and coworkers have studied the properties of polyurethane zwitterionomers[50–54]. In their work, γ-propane sultone was reacted with the tertiary amine in the backbone of the chain extender (n-methyldiethanolamine) to create a zwitterionomer, with the backbone nitrogen becoming a quaternary ammonium (charge +1) attached through three methylene groups to an $-SO_3^-$ group. It was found that, at constant hard-segment content, microphase separation improves and the rubbery plateau shifts to higher modulus values and extends to higher temperatures. These zwitterionomers were also converted to anionomers by removing the pendant methyl group from the backbone nitrogen during neutralization of the $-SO_3^-$ group with metal acetates[53]. The metal acetates used were sodium acetate trihydride, zinc(II) diacetate dihydride and iron(III) diacetate hydroxide. It was found that when the hard segments are interconnected due to high hard-segment content, the rubbery plateau increases with increasing cation charge. As the hard-segment content decreases and the hard phase becomes more dispersed, cation charge has little effect on the rubbery plateau. Improving the hard domain cohesiveness through ionic crosslinking obviously has more of an effect if these domains are interconnected.

In all of the materials discussed to this point, the ionic groups have been distributed in a random fashion along the polymer chain. Neutralization of these ionic groups then results in a rather ill defined network in which the molecular weight between crosslinks may vary greatly. Also, the presence of dangling or free chain ends will have a deleterious effect on properties in the rubbery region. As mentioned earlier, another approach is to prepare telechelic ionomers which have the ionic groups located only at the chain ends. This well defined chain microstructure should then lead to an ionic network which is much better defined than those formed by the traditional ionomers. This approach was first pursued by Otocka *et al.*[55], who studied the bulk and solution viscosity of carboxy-terminated polybutadiene in both the unneutralized and neutralized forms. More recently, extensive research on telechelic ionomers has been conducted by Broze, Jérôme, Teyssié and coworkers[56-67] and by Wilkes, Kennedy and coworkers[68-78].

The work of Broze, Jerome, Teyssie and coworkers has been focused on linear carboxylated telechelic ionomers based primarily on either polybutadiene or polyisoprene. They have studied the solution behaviour of these materials[56,59-61] as well as their higher-temperature bulk properties[57,58,62-67]. It was found that for ion concentrations below 0.7 mol% (or $\bar{M}_n > 2 \times 10^4$), the relaxation obeys a Williams–Landel–Ferry (WLF) type of dependence. However, the time–temperature superposition principle fails at higher ion concentration (or lower $\bar{M}_n$). These workers have also neutralized these materials with higher-valency cations such as titanium(IV) and zirconium(IV). Recent studies of the mechanical properties of these materials by Tant *et al.*[79] suggest that the carboxylated telechelic ionomers are generally weaker than the sulphonated telechelic ionomers, as would be expected based upon the work of Lundberg and Makowski[32].

As mentioned earlier, we have taken the approach of synthesizing sulphonated polyisobutylene telechelic ionomers with a broad range of molecular architectures—linear monofunctional, linear difunctional and three-arm star trifunctional. The solid-state mechanical properties[68-73,75], melt rheological properties[74,75] and solution properties[77,78] of these materials have been investigated. In this paper, we present the results of extensive studies of the solid-state mechanical properties of these materials. The variables which are considered include (1) molecular weight and its distribution, (2) molecular architecture, (3) type of neutralizing cation, (4) type of counteranion (e.g. $Ca(OH)_2$ vs. $CaAc_2$), and (5) excess neutralizing agent. To a more limited extent, the effects of moisture, addition of an ionic plasticizer and thermal recycling are also considered. Bulk properties of interest include stress–strain behaviour, stress relaxation, permanent set, mechanical hysteresis, dynamic mechanical and thermomechanical behaviour.

EXPERIMENTAL

Materials

Synthesis. Recent insight into the mechanism of carbocationic olefin polymerization has led to the synthesis of olefin telechelic polyisobutylene (PIB), i.e. PIB carrying $-CH_2-C(CH_3)_2=CH_2$ end groups. The synthesis and characterization of these linear telechelic (α,ω-difunctional) polyisobutylenes has been described previously[80-86]. The synthesis involved the use of difunctional initiator chain transfer agents known as inifers. For example, the use of the *p*-dicumyl chloride/BCl_3 inifer system led to the preparation of polyisobutylenes carrying two $-CH_2-C(CH_3)_2Cl$ termini with a functionality of 2.0. Dehydrochlorination of these polyisobutylenes with a hindered base quantitatively yielded α,ω-diolefins[83]. This same concept used for the synthesis of linear telechelics was extended to the preparation of three-arm star telechelic polymers by Kennedy *et al.*[82] Similarly to the synthesis of linear telechelic PIB dichlorides with the bifunctional inifer (binifer) *p*-dicumyl chloride, the three-arm star telechelic polyisobutylene trichlorides were obtained by the use of the symmetrical tricumyl chloride (TCC)/BCl_3 'trinifer' system. Subsequent quantitative dehydrochlorination of the telechelic PIB trichlorides with the hindered base t-BuOK under appropriate conditions led to the formation of the olefinic form of the three-arm star polyisobutylenes. Similarly, the monofunctional form of the olefinic linear PIB was synthesized using a monocumyl chloride/BCl_3 (unifer) initiator. Experimental details of the synthesis and purification of these materials have been discussed by Storey[86].

Sulphonation. Heterogeneous sulphonation was carried out in hexane solutions at room temperature. Five grams of the chloride form were dissolved in about 50 ml of hexane at room temperature. Then 1.4 ml of acetic acid were added with stirring, and after 10 min 0.67 ml of sulphuric acid was added. After stirring for 2 h the mixture was allowed to separate and the lower sulphuric acid layer was discarded. The sulphonated product was isolated and then purified. Since the acid form is unstable at room temperature, it was then stored in a freezer until neutralized with various bases. Experimental details have been discussed by Storey[86].

Neutralization. The neutralization procedures have been described in detail previously[72]. Neutralization of the acid form was carried out in tetrahydrofuran (THF). The acid was titrated using classical techniques and indicators. For cases in which the neutralizing agent was a weak base, thereby making direct titration difficult, aliquots were titrated with a strong base to determine the normality of the acid solution. Then an equivalent normal amount of the weak base was added to the unneutralized solution for stoichiometric neutralization. Following neutralization, antioxidant (Irganox 1010) was added and films were cast in Teflon moulds. These films were then dried in a vacuum oven at 80°C for at least 24 h.

Chemical structure and nomenclature. The sulphonated polyisobutylene (PIB) telechelic ionomers were prepared in the following three molecular architectures: linear monofunctional, linear difunctional and three-arm star trifunctional. The chemical structures are illustrated in *Figure 1*. The terminal sulphonic acid groups were neutralized with bases such as potassium hydroxide, calcium hydroxide and zinc acetate. The nomenclature used is best described by an example. The designation T-14-K-0 refers to the trifunctional ionomer of 14 000 M_n neutralized with KOH to the endpoint (0% *excess*). The cation standing alone (e.g. T-14-Ca-0) indicates that the hydroxide form was used. When in conjunction with 'Ac' (e.g. T-14-CaAc-0), then the acetate form was used.

Film preparation. The neutralized materials were compression moulded at 150–160°C for about 5 min to form films from which samples were cut. For the materials with greater than the stoichiometric amount of neutralizing agent, slightly higher temperatures or slightly longer moulding times were required to prepare uniform films.

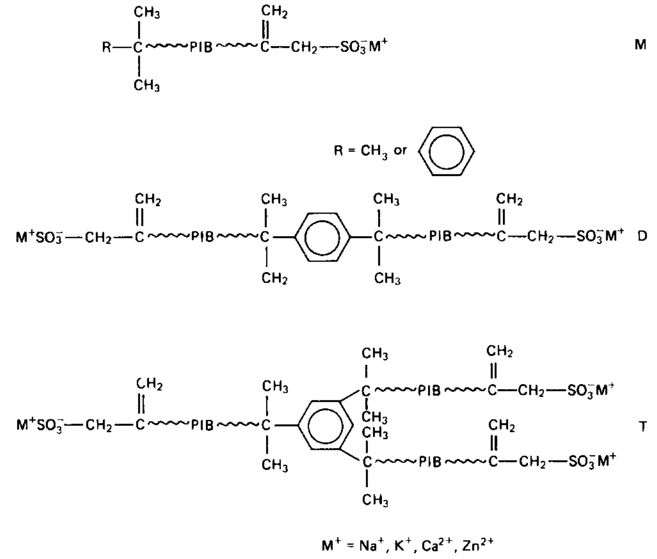

Figure 1 Chemical structure of the sulphonated polyisobutylene telechelic ionomers (M = monofunctional, D = difunctional and T = trifunctional)

Techniques

Small-angle X-ray scattering (SAXS). Small-angle X-ray scattering was used to investigate qualitatively the presence or absence of clusters in several of these ionomers. A standard Kratky small-angle X-ray camera was utilized for the SAXS experiments. The X-ray source was a Siemens AG Cu 40/2 tube operated at 40 kV and 20 mA by a GE XRD-6 generator. Cu Kα radiation of wavelength 1.542 Å was obtained by a Ni-foil filter. The scattered intensity was monitored by a one-dimensional Braun position-sensitive detector from Innovative Technologies Inc. In addition, some SAXS experiments were performed on selected samples by Dr C. W. Williams using the synchrotron facility at Stanford University.

Wide-angle X-ray scattering (WAXS). Wide-angle X-ray scattering experiments were performed to study the phenomenon of strain-induced crystallization. A Phillips table-top X-ray generator model PW1170 was utilized with a standard vacuum Statton photographic camera. An exposure time of about 16 h was typically used on samples about 10–15 mils (0.25–0.38 mm) thick.

Infra-red spectroscopy. A Nicolet MX-1 infra-red spectrophotometer with Fourier transform capabilities was used to investigate the presence of moisture in these materials.

Mechanical properties. Microdumbbells 10.0 mm long were cut from the compression-moulded films for mechanical property studies. Stress–strain experiments were performed using an Instron model 1122 and were conducted at room temperature at an initial strain rate of 100% min^{-1}. Instantaneous set was determined by cyclic loading and unloading at the same rate to increasing strain levels in increments of 50% elongation. The end of the unloading cycle and the beginning of the next loading cycle was taken as the point when stress reached zero. The instantaneous set was defined as the elongation at the end of each cycle. The per cent hysteresis for a given cycle was calculated as the area bounded by the loading–unloading curves to the total area under the loading curve multiplied by 100. These areas were determined using an electronic digital planimeter. Stress relaxation experiments were carried out on a Tensilon model VTM-II (Toyo Measuring Instruments Co.), owing to the excellent stability of this instrument over long periods of time. Samples were strained at a rate of 400% min^{-1} to either 25% or 100%. Stress-relaxation experiments at temperatures above room temperature were performed using the static mode of a Rheovibron model DDV-IIC.

Thermal properties. Thermomechanical analysis. (t.m.a.) was performed using a Perkin–Elmer TMS-2. The temperature range from −100°C to softening (up to 300°C) was scanned at a heating rate of 10°C min^{-1}, and the penetration of a probe under a 10 g load was monitored. T.m.a. experiments were performed under a nitrogen atmosphere.

RESULTS AND DISCUSSION

Qualitative SAXS analysis

SAXS experiments were performed on both the three-arm star trifunctional and linear difunctional ionomers. *Figure 2* shows the smeared data of the scattered intensity as a function of scattering angle for T-19-Ca-100. The intensity decreases monotonically with increasing scattering angle with no sign of an 'ionic peak'. As discussed earlier, the presence of a low-angle scattering peak is considered to be evidence of a cluster morphology. The SAXS data thus suggest the absence of any significant degree of 'periodic' clustering in this material, probably because of the low ionic content. Thus it is believed that the predominant type of ionic association in this material is the multiplet.

Recent work on lower-molecular-weight three-arm star trifunctional and linear difunctional ionomers has revealed that these materials do indeed display a broad low-angle SAXS peak when $\bar{M}_n$ is less than about 10 000. Of course, these lower-molecular-weight materials also have a higher ionic content, and thus the formation of clusters would be more probable. As mentioned earlier, clustering is normally found to occur at a certain critical ionic content which is dependent upon both the polymer backbone type as well as the type of ionic group. The

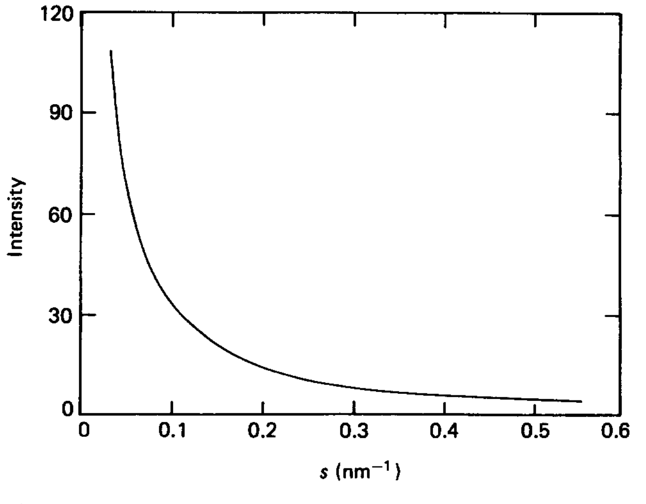

Figure 2 Smeared SAXS intensity vs. scattering vector for T-19-CaAc-100

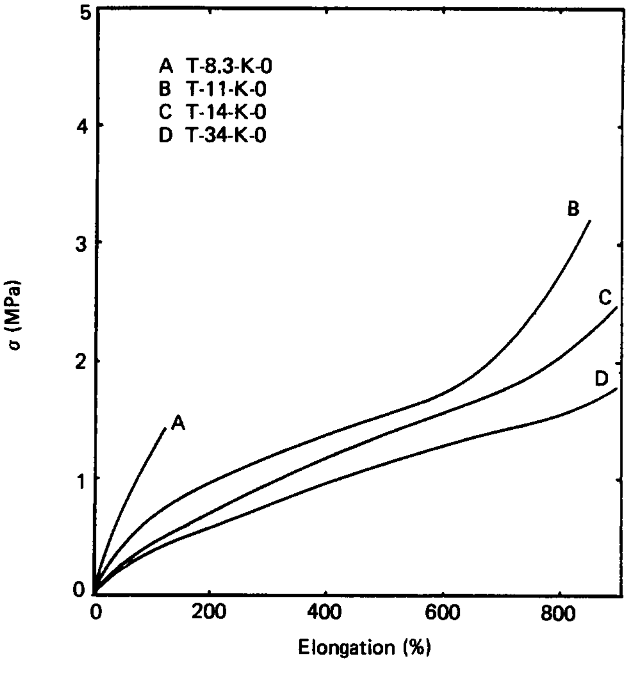

Figure 3 Effect of molecular weight on stress–strain behaviour of T-X-K-0 series

results of the SAXS studies will be the topic of a separate paper[87].

Mechanical behaviour of three-arm star trifunctional species

Effect of molecular weight. The effect of molecular weight on the stress–strain behaviour of the trifunctional ionomers is illustrated in *Figure 3*. Data for T-8.3-K-0, T-11-K-0, T-14-K-0 and T-34-K-0 are shown. The T-8.3-K-0 sample displays a rather low extension at break (~150%) which is not very characteristic of elastomers. The reason for this is not yet completely clear, although the probable explanation is that the low extension results from a higher ionic crosslink density. It is also noted that T-8.3 is the only sample in this series which showed a broad SAXS peak. For some of the higher-molecular-weight materials extensions as high as 1350% have been observed, although ultimate extensions of 800–1000% are more common. Many of these samples broke at the clamps of the Instron, thereby reducing the ultimate elongation.

According to the stress–strain data shown in *Figure 3*, stress decreases with increasing molecular weight at any given elongation. To a first approximation, this can be explained by the simple Gaussian theory of rubber elasticity, where the engineering stress, σ, is given by:

$$\sigma=\frac{\rho RT}{M_c}\left(\lambda-\frac{1}{\lambda^2}\right) \qquad (1)$$

where ρ is the density of the material, R is the universal gas constant, T is the absolute temperature and M_c is the number-average molecular weight between crosslinks. The extension ratio, λ, is defined as l/l_0, where l is the deformed length and l_0 is the initial undeformed length. If it is assumed that only two ion pairs associate to form a multiplet, then M_c would be equal to the average molecular weight of two arms, i.e. $M_c=\frac{2}{3}\bar{M}_n$. Thus, M_c decreases with decreasing $\bar{M}_n$ and the stress, according to equation (1), must therefore increase. This is the observed behaviour.

In the derivation of equation (1) affine deformation is assumed, i.e. the ratio of the microscopic deformations to the macroscopic deformation is unity. However, recent work suggests that the elongation of a network can be represented as affine probably only in the range of deformations that are less than 50%[88]. At higher deformations it is thought that junction fluctuations diminish the modulus by a factor of less than 1, this factor being dependent upon the functionality of the network junction point[89]. In the limit of large deformations, the non-affine deformation behaviour is exhibited by a 'phantom' network, where the network chains are portrayed as being able to pass freely through one another. In this study, we have utilized stress-relaxation experiments at lower elongations to minimize deviation from Gaussian behaviour as well as problems arising from strain-induced crystallization (if present) and other energetic effects that would undermine the Gaussian approximation. It should also be pointed out that equation (1) was derived utilizing equilibrium thermodynamics, whereas the stress–strain experiment is a non-equilibrium process. Thus the effective M_c determined from stress–strain data will be affected by molecular frictional effects and temporary crosslinks resulting from entanglements. These effects will be addressed shortly.

Stress relaxation curves for T-11-K-0, T-14-K-0 and T-34-K-0 at 25% and 100% elongations are shown in *Figure 4*. These materials reach a near plateau stress after about 1 h. The plateau stress level decreases in the order T-11>T-14>T-34 as would be predicted from equation (1). The plateau stress is 50% to 80% of the initial stress in all cases. It is clear from the stress-relaxation data that these materials do not behave as perfectly linear viscoelastic materials, i.e. the ratio of stress at 100% elongation to that at 25% elongation is not constant at all times for a given polymer. However, this is not uncommon for elastomers at these extensions. It should also be pointed out that a true equilibrium stress is not reached due to 'ion hopping' as discussed by Hara *et al.*[90] In fact, long-term stress-relaxation and creep experiments on these materials by Tant *et al.*[76] have

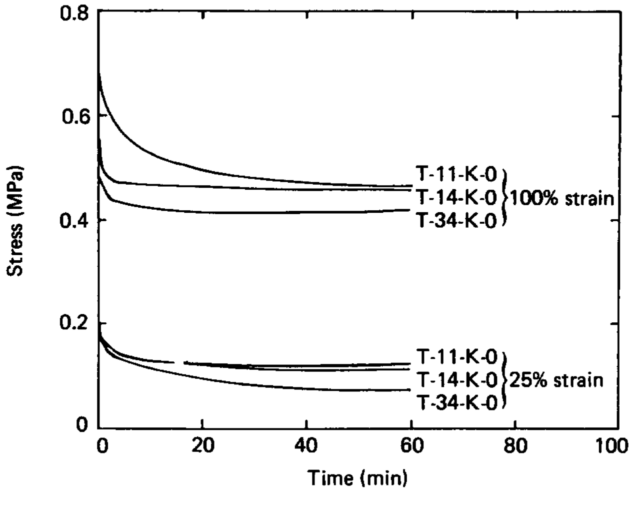

Figure 4 Effect of molecular weight on stress-relaxation behaviour of T-X-K-0 series

Table 1 Effective molecular weight between 'crosslinks' (M_c) calculated by different routes for the T-X-K-0 systems having different molecular weights

Material	M_c (stress–strain)	M_c (stress-relax.)	M_c (2 × arm mol. wt.)
T-11-K-0	5800	11300	7300
T-14-K-0	8800	12100	9300
T-21-K-0	8100	15000	14000
T-34-K-0	8700	18400	22700

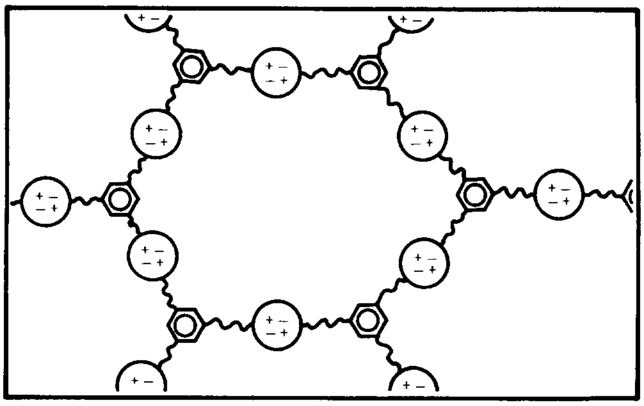

Figure 5 A simple morphological model for end-linked tri-arm ionomer neutralized stoichiometrically

shown that an apparent change in relaxation mechanism occurs at much longer times (about 1 week) resulting in significant further relaxation. However, it is still believed that the apparent equilibrium stress that is reached after 1–2 h of relaxation is the appropriate stress to use in calculating an effective M_c for the ionic network. The M_c values calculated in this way are given in *Table 1*.

If one assumes affine behaviour with a Poisson ratio of 0.5, then M_c can be calculated using the equation:

$$E = 3\frac{\rho RT}{M_c} \tag{2}$$

where E is Young's modulus or the initial slope of the stress–strain curve. Using this equation and the stress–strain curves from *Figure 3*, effective molecular weights for the same series were calculated and are also given in *Table 1*. This table also contains the theoretical M_c values calculated by assuming that only two ion pairs associate, i.e. $M_c = \frac{2}{3}\bar{M}_n$. It is seen that the M_c values calculated from stress–strain data are all significantly lower than those calculated from the stress-relaxation data. This strongly suggests that there are entanglement or frictional non-equilibrium effects contributing to the initial modulus in these materials as would be expected, and which lead to a lower value of M_c estimated by this method. On the other hand, in the stress-relaxation experiment these effects are minimized. It is interesting that the estimated values of M_c from the stress-relaxation experiments and those calculated theoretically ($M_c = \frac{2}{3}\bar{M}_n$) are in quite good agreement. This leads to the tentative hypothesis that there are, on average, two ion pairs per multiplet in these materials. If there were an average of more than two ion pairs per multiplet, then the molecular weight between network junction points would be less. In fact, for multiplet functionality being three or higher, the M_c would be equal to the molecular weight of one arm ($M_c = \frac{1}{3}\bar{M}_n$), which clearly is not in agreement with the results. A simple morphological model, shown in *Figure 5*, is therefore postulated in which only two ion pairs associate to form a multiplet. While this is probably an oversimplification, it does account for the mechanical data.

From equation (1), if stress, σ, is plotted vs. $(\lambda - 1/\lambda^2)$, then the curve should be linear with a slope of $\rho RT/M_c$ provided the network behaves in a Gaussian manner. Although equation (1) is valid only under equilibrium conditions, we have plotted stress–strain data for some of the materials in this manner. Specifically, the curves for T-14-K-0, T-14-Ca-0 and T-14-Ca-125 are shown in *Figure 6*. These curves are seen to be quite linear up to an extension of about 500%. Thus these materials behave in a very Gaussian rubber-like manner even under these non-equilibrium conditions at relatively high extensions. An interesting feature is the upturn in stress at about 550% extension which suggests either the development of crystallinity at higher elongations or deviations from Gaussian behaviour due to limited chain extensibility. The presence of crystallinity at high extensions has been confirmed by WAXS and will be discussed later. Theoretical calculations to estimate the maximum chain extensibility for different molecular-weight systems have also been performed. Surprisingly, the theoretically calculated values of maximum chain extensibility are somewhat lower than those observed experimentally. However, the calculations are based on linear PIB and thus may not directly apply in this case for the three-arm star systems. It may be suspected that the observed high extensions may be due to ion hopping, but hysteresis

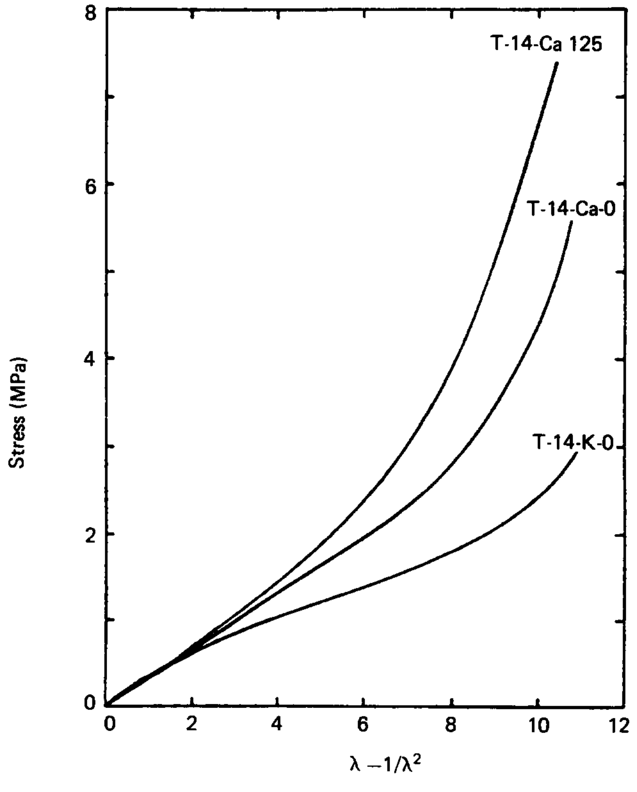

Figure 6 Rubber elasticity plot for T-14-K-0, T-14-Ca-0 and T-14-Ca-125

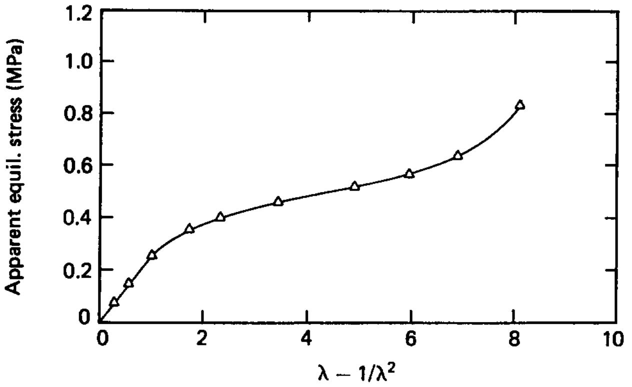

Figure 7 Equilibrium rubber elasticity plot for T-14-K-0

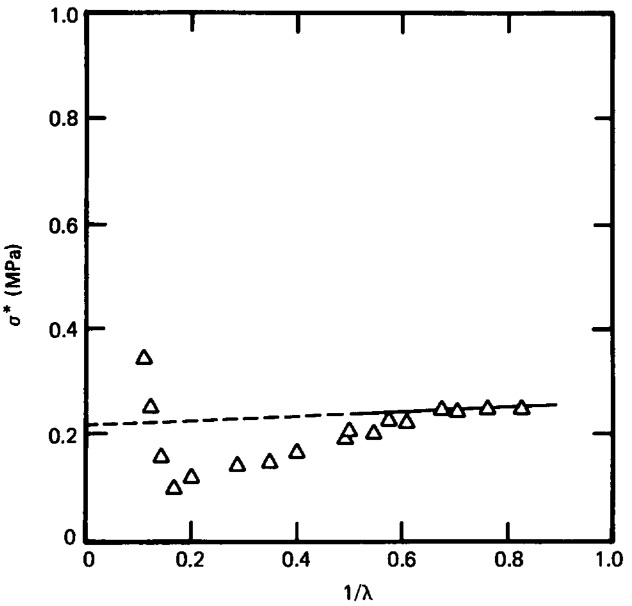

Figure 8 Mooney–Rivlin plot for T-14-K-0

and permanent set data to be presented later do not support this.

Much of this discussion has been focused on the non-equilibrium stress–strain behaviour of the materials. In order to investigate their network character further, stress-relaxation experiments were conducted on T-14-K-0 at different levels of strain. The apparent equilibrium stress values were obtained after about 2 h at each extension. The resulting data are shown as a rubber elasticity plot, σ vs. $(\lambda - 1/\lambda^2)$, in *Figure 7*. The molecular weight between crosslinks, M_c, was calculated from the initial slope of this curve using equation (1). A value of about 9300 was calculated, which agrees with the stress-relaxation results discussed earlier.

Another way of analysing the equilibrium stress–strain behaviour of rubber networks is the semi-empirical equation of Mooney and Rivlin[91,92]. The equation of state is:

$$\sigma = 2C_1 + \frac{2C_2}{\lambda}\left(\lambda - \frac{1}{\lambda^2}\right) \qquad (3)$$

where $2C_1$ and $2C_2$ are constants independent of λ. In the limit of large deformations $(1/\lambda \rightarrow 0)$ the constant $2C_1$ can be related to M_c. The constant $2C_2$ is regarded as a measure of the deviation from Gaussian behaviour. A Mooney–Rivlin plot, $\sigma/(\lambda - 1/\lambda^2)$ vs. $1/\lambda$, is shown in *Figure 8* using the apparent equilibrium stress data for T-14-K-0. According to the Mooney–Rivlin equation, this plot has an ordinate intercept of $2C_1$ and a slope of $2C_2$. Again the upturn in stress is due to strain-induced crystallization. At lower deformations, the curve is fairly linear and the intercept and slope have been determined by linear regression. Although there is some scatter in the data, the value of M_c estimated from the intercept is about 10 200. This is still in reasonable agreement with the value obtained from the rubber elasticity plot in *Figure 7*. Again, if it is assumed that two ion pairs associate to form each multiplet, then for T-14-K-0 the M_c should be ~9300. The values of M_c determined from the rubber elasticity plot and the Mooney–Rivlin plot agree quite well. Since the slope of the Mooney–Rivlin plot is non-zero, it is apparent that there is some deviation from Gaussian behaviour as is typical for various kinds of elastomers. Therefore the results of this analysis should not be considered exact, but should be regarded as an estimate of M_c.

A good elastomer should be able to sustain large deformations and also display good recovery (low permanent set) and low mechanical hysteresis. The instantaneous set behaviour of T-8.3-K-0, T-11-K-0, T-14-K-0 and T-34-K-0 is shown in *Figure 9*. It should again be noted that the instantaneous set is the per cent elongation (based on the initial length before deformation) at the time when stress becomes zero as the crosshead is in its return cycle. The instantaneous set of these materials is relatively small, being only 50–60% even after 700% elongation which includes 14 deformation cycles. Additional recovery is also observed with longer times. In order to investigate the long-term

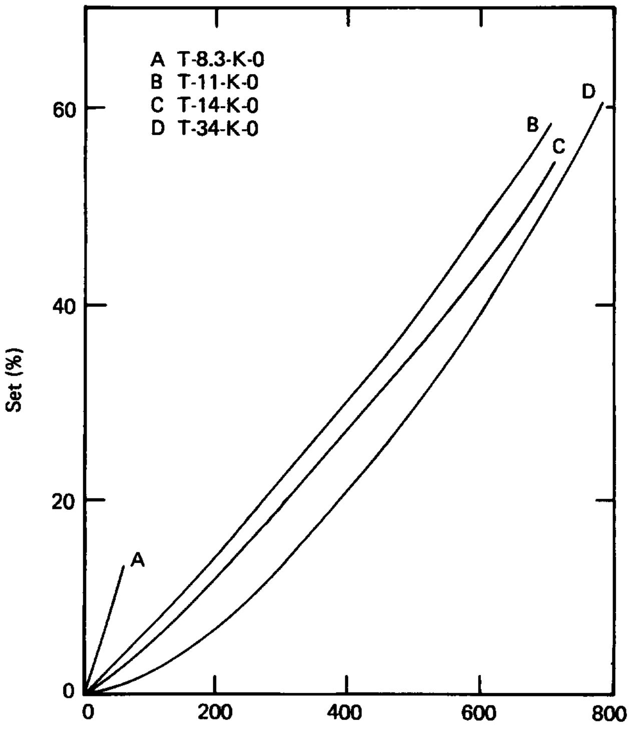

Figure 9 Per cent set vs. elongation for T-X-K-0 series

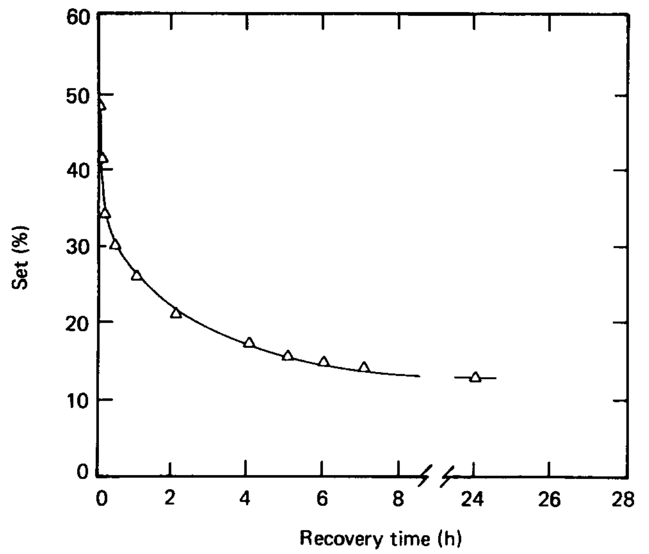

Figure 10 Recovery of T-34-K-0 following 700% extension for 24 h

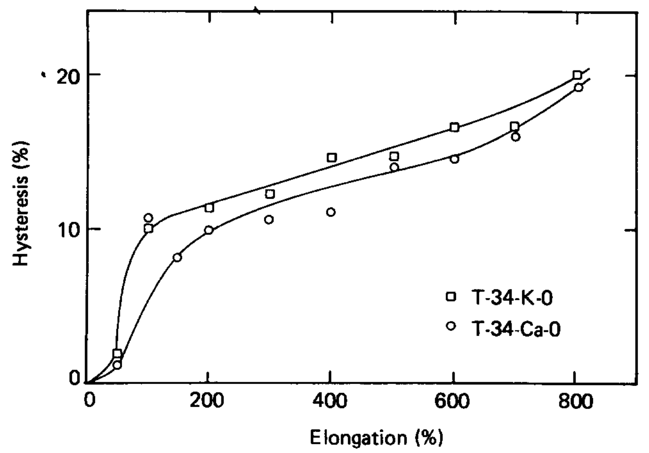

Figure 11 Mechanical hysteresis vs. elongation for T-34-K-0 and T-34-Ca-0

stability of one of these materials under deformation, a sample of T-34-K-0 was held at 700% elongation at ambient temperature for a period of 24 h and the subsequent recovery after removal of the load was observed as a function of time. The results, shown in *Figure 10*, indicate that after 24 h of recovery the set is only 13% of its initial undeformed length. This additional recovery with time clearly implies good network integrity with little ion hopping. Similar results were obtained following 24 h deformations at lower extensions. Longer-term permanent set measurements and their temperature dependence are now under way and will be reported in the near future.

The mechanical hysteresis response of T-34-K-0 and T-34-Ca-O is shown in *Figure 11*. The per cent hysteresis reaches only 20% at elongations of 800%. This is quite low considering that these polymers are not covalently crosslinked, are of relatively low molecular weight, and the experiments are performed well above T_g ($\sim -65°C$). Obviously, very little energy is lost in deforming these materials, most of the energy being recovered upon unloading. Furthermore, the mechanical hysteresis of these materials is much lower than for many other thermoplastic elastomers such as SBS block copolymers and polyurethanes. (It is realized that the content of the 'hard phase' in the latter systems is important when considering mechanical hysteresis or permanent set.)

In order to test the reproducibility of stress–strain data and to determine the effects of thermal compression moulding, a particular sample of T-11-K-100 was compression-moulded five times. Each moulding cycle consisted of holding the material at 150°C for 15 min. Stress–strain experiments were conducted after each moulding. No change in stress–strain behaviour was noted as a result of this thermal recycling. Thus, from the results presented, it may be concluded that, except for T-8.3-K-0, the three-arm star ionomers are surprisingly good thermoplastic elastomers, especially considering that they are of low molecular weight with only three ionic groups per molecule.

Strain-induced crystallization. It was mentioned earlier when discussing the stress–strain curves in *Figure 3* that the upturn in stress at high extensions is due to strain-induced crystallization. This upturn in stress is also clear in the rubber elasticity and Mooney–Rivlin plots of *Figures 7* and *8*, respectively, for T-14-K-0. In order to confirm the presence of strain-induced crystallinity in these materials, wide-angle X-ray scattering patterns were taken at three different fixed elongations (400%, 575% and 975%) for T-11-Ca-100. These WAXS patterns are shown in *Figure 12*. The pattern obtained at 400% elongation is a diffuse amorphous halo, indicating the absence of any significant crystallinity. However, upon

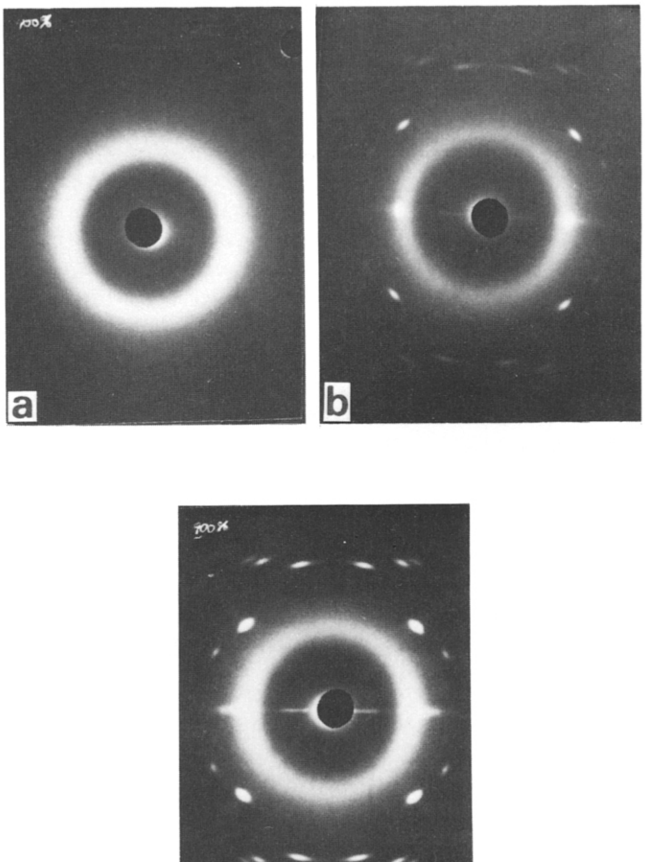

Figure 12 WAXS patterns for T-11-Ca-100 at (a) 400%, (b) 575% and (c) 975% elongation

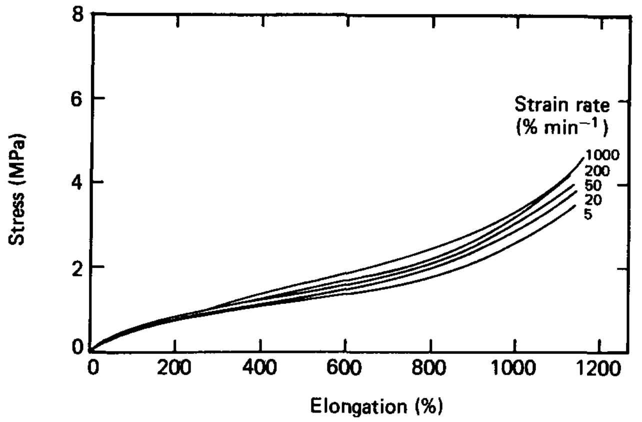

Figure 13 Effect of strain rate on the stress–strain behaviour of T-34-K-0

extension to 575% a sharp diffraction pattern is observed, indicating the presence of a pronounced oriented crystalline morphology superimposed on the diffuse scattering from a still highly amorphous system. Upon further stretching the sample to 975% the diffraction pattern becomes still sharper, indicating increased crystallinity, but clearly a considerable amorphous content remains. The pronounced azimuthal dependence of the WAXS patterns suggests that the crystals formed are highly oriented. The crystals act as physical crosslinks, further strengthening the network at higher extensions and enhancing the tensile properties. Furthermore, the crystallites are reversible in that they melt out upon unloading, thereby permitting good recovery.

The extension at which the upturn in stress is observed is slightly affected by the rate of deformation. To investigate this effect, the stress–strain behaviour of T-34-K-0 was studied at initial strain rates ranging from 5 to 1000% min^{-1}. The results are shown in *Figure 13*. The initial slope, corresponding to Young's modulus, does not significantly change with strain rate. However, the relative elongation at the onset of the upturn in stress decreases with increasing strain rate. This suggests that at higher strain rates the molecules have less time to relax partially, and consequently their increased molecular orientation at higher strain rates leads to crystallization at lower extensions. The fact that there is very little dependence upon strain rate indicates that the behaviour is dominated by ionic crosslinking effects rather than entanglements. If entanglement effects controlled the behaviour, there would be a significant dependent of the stress–strain behaviour upon the strain rate. At lower strain rates the entanglements would have more time to disentangle and reduce the stress. At higher strain rates the entanglements would be felt as crosslinks. Thus the effective crosslink density would depend upon strain rate and the stress would be strongly affected.

Effect of excess neutralizing agent. During the course of this investigation it was found that adding excess neutralizing agent during the neutralization step greatly affects the mechanical properties of these ionomers[72]. In the past, other workers have often added excess neutralizing agent, assuming that the excess is then washed out by using simple purification procedures. To check this assumption, a series of the T-14 ionomer was prepared with different amounts of KOH ranging from 90% neutralization (−10% excess) to 300% excess. The ionomer/THF solutions were then 'stream stripped' by pouring slowly into boiling distilled water (about 1 litre boiling water per 5 ml solution). The precipitated ionomers were further washed by stirring in 1 litre of boiling distilled water for 30 min, followed by two more washings in boiling distilled water.

The stress–strain behaviour of this series is shown in *Figure 14*. It is clear that the ionomer must be fully neutralized to obtain reasonable properties, since the ionomer which was only 90% neutralized displayed a much lower modulus and stress. This is expected since the number of crosslinks should be reduced. Also, the unneutralized sulphonic acid groups may degrade upon compression moulding at 150°C, thus resulting in further defects in the network and a reduction in the number of crosslinks. Stoichiometric neutralization increases Young's modulus, the ultimate extension and the ultimate stress. As given in the figure, the modulus of the T-14-K-(−10) material is 0.5 MPa, while for the stoichiometric and excess neutralized materials it ranges from 0.8 to 0.95 MPa. The per cent excess neutralizing agent is also seen to strongly affect stress–strain behaviour. Clearly, the attempts to remove the excess neutralizing agent, even though the treatments were very harsh, were not successful. Young's modulus varies little with excess neutralizing agent. Since this value is related to M_c, the number of crosslinks should remain relatively constant. However, the ultimate properties are very sensitive to the amount of excess neutralizing agent. Based on these two factors, we have postulated the simple morphological model shown in *Figure 15*. It is suggested that the excess neutralizing agent is not distributed uniformly throughout the material, but is preferentially attracted to the regions of high dielectric constant—the ionic multiplets. Apparently, the excess neutralizing agent strengthens the ionic aggregates and helps to prevent ion hopping. This then helps to strengthen and stabilize the network structure. It should be mentioned that these effects on mechanical properties due to excess neutralizing agent have also been observed with other cations such as calcium and zinc[93].

Our proposed morphological model is also supported by long-term permanent set data. Again, these data were

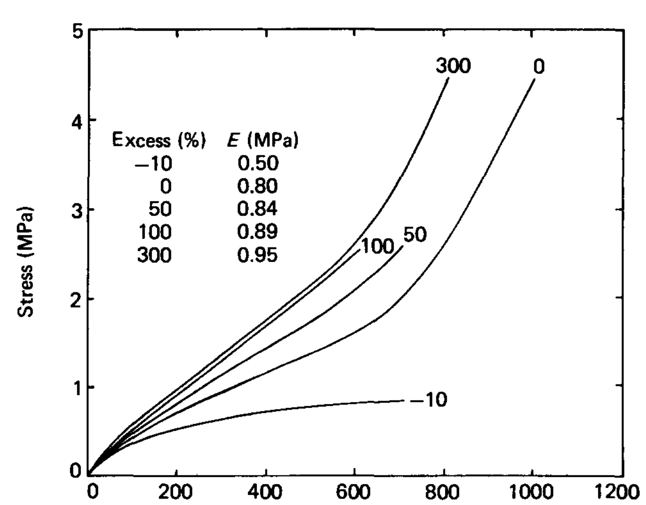

Figure 14 Effect of excess neutralizing agent on the stress–strain behaviour of the T-14-K series

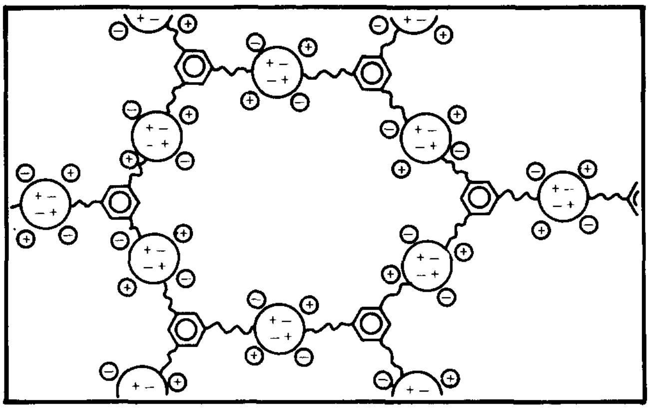

Figure 15 Simple morphological model for the tri-arm system containing excess neutralizing agent

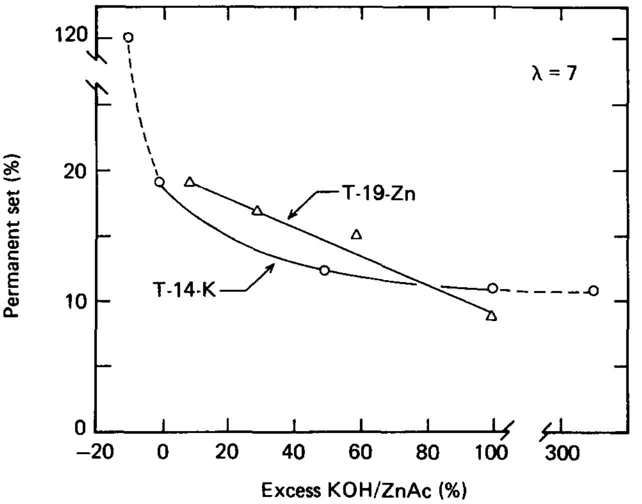

Figure 16 Effect of excess neutralizing agent on the permanent set of the T-14-K and T-19-Zn materials following 700% elongation for 24 h. Permanent set was recorded following 24 h of recovery

obtained by extending the material to 700% and maintaining the deformation for 24 h. The stress was then removed, and permanent set was noted after 24 h of recovery. These data are given as a function of per cent excess neutralizing agent for the T-14-K and T-19-Zn series in *Figure 16*. In both series the recovery improves with excess neutralizing agent. Apparently, the excess neutralizing agent reduces ion hopping, thus improving the long-term integrity of the network.

Increasing the number of ionic species within the ionic multiplets by addition of excess neutralizing agent apparently increases the coulombic forces of attraction and therefore the energy required for ionic dissociation. Consequently, it would be expected that higher temperatures would be required to relax or weaken the ionic crosslinks. This is verified by the thermomechanical analysis (t.m.a.) results presented in *Figure 17*. The softening temperature following the rubbery plateau for T-14-K-(−10) is only 60°C. Complete neutralization extends this plateau to about 100°C. With addition of excess neutralizing agent the rubbery plateau is extended to higher temperatures, finally reaching about 160°C for the T-14-K-300 material. These results lend further support to the simple morphological model presented earlier.

Again, the common assumption that a simple washing purification procedure removes excess neutralizing agent is not correct. It has been suggested that the observed behaviour might instead be due to the removal of associated water from the multiplets. However, information obtained from infra-red spectroscopy, which is not presented here, does not support this speculation.

Effect of cation type. Another important variable which may affect the properties of ionomers is the type of cation used to neutralize the acid precursor. Because of limited quantities of the materials of interest here, only potassium, calcium and zinc cations have been utilized to date. Stress–strain curves for the T-34-K-100, T-34-Ca-100 and T-34-Zn-100 materials are shown in *Figure 18*. The T-34-Zn-100 material has properties comparable to the T-34-Ca-100 material, and both of these display higher stresses than T-34-K-100 at high elongations. It is interesting to note that T-34-Ca-100 (neutralized with divalent calcium) has a higher tensile strength than T-34-K-100 (neutralized with monovalent potassium). Yet both calcium and potassium are highly ionic in character, in contrast to the transition-metal zinc, which forms

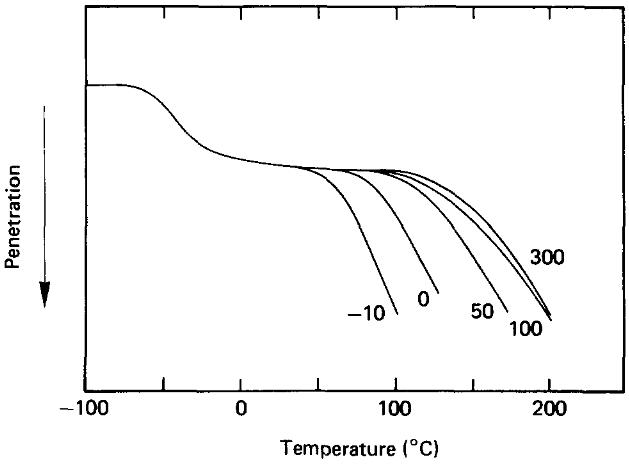

Figure 17 Effect of excess neutralizing agent on the thermomechanical behaviour of the T-14-K series

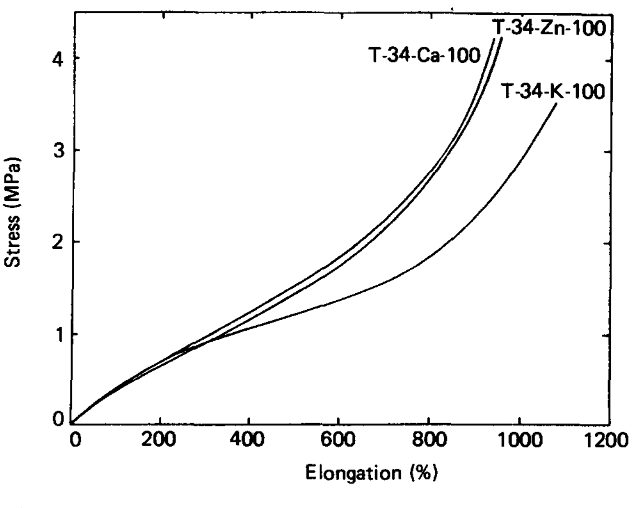

Figure 18 Effect of cation type on the stress–strain behaviour of the T-34-X-100 series

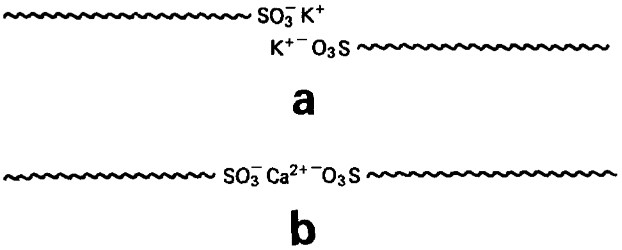

Figure 19 Schematics of ionic crosslinking for (a) monovalent and (b) divalent cations

bonds of more covalent character. Matsuura and Eisenberg[94] have suggested that the ionic potential, q/a (q = charge, a = ionic radius), of the cation is a very important parameter in determining the effect of cation type on the properties. Specifically, in several ethyl acrylate ionomer systems it was observed that ionomers neutralized with lithium had the highest ionic association, followed by sodium and caesium in accordance with their decreasing ionic potential.

Likewise, in these PIB telechelic ionomers the ionic potential of divalent calcium is higher than that for monovalent potassium. If one assumes only ion pair association at the chain ends, then the ionic bonding for the monovalent and divalent cations could be of the type shown in *Figure 19*. As a first approximation, the lattice energy of potassium sulphate and calcium sulphate should give an indication of the energy required to disrupt these ionic bonds. Indeed, the lattice energy of potassium sulphate (530 kJ mol^{-1}) is much lower than that for calcium sulphate (1300 kJ mol^{-1}). It may then be expected that the energy of ionic association would be greater in calcium-neutralized ionomers than in the corresponding potassium-neutralized ionomers. The observed mechanical behaviour lends support to this argument. However, it has been suggested by Bagrodia and Wilkes[95] that the concept of ionic potential satisfactorily explains the effects of cation type only when the cations belong to the same group of the periodic table (or have similar ionic character). The electronic configuration of the cation, which governs its covalent character, is believed to be a very important factor in determining the properties of ionomers. In support of this contention, it has been observed that the melt viscosity of the PIB telechelic ionomers neutralized with zinc is much lower than for the corresponding materials neutralized with potassium and calcium cations[75]. Likewise, from t.m.a. studies it was found that the softening temperature following the rubbery plateau was lowest for the zinc-neutralized ionomers. Thus, it appears that the zinc-neutralized ionomers would be more easily processed than those neutralized with potassium or calcium.

The effect of the counteranion associated with the cation was also studied to a very limited extent. The T-34 ionomer was neutralized with both calcium acetate and calcium hydroxide. The stress–strain behaviour and softening temperatures of the two resulting materials were found to be essentially the same. These experiments are not, of course, sufficient to make any broad generalizations regarding the effect of counteranion.

Effect of bimodal distribution. Llorente, Andray and Mark[96–98] have recently focused attention on the non-Gaussian behaviour related to chain extensibility in elastomeric networks. They investigated the elastomeric properties of polydimethylsiloxane (PDMS) networks having a bimodal distribution consisting of very short (M_n = 220 or 660) and relatively long (M_n = 18 500) chains. An interesting feature of these systems is that they do not crystallize upon high extension. Thus their non-Gaussian behaviour could be studied without the complications of strain-induced crystallization. It was found that the ultimate property of tensile strength increases significantly over that for the individual components. This behaviour was attributed to extensive redistribution of strain within the network structure so as to avoid any network chains being stretched to their maximum lengths. Llorente and Mark[97] extended this study by using short PDMS chains (M_n = 1100) and long PDMS chains (M_n 18 500). Although similar results were obtained, it was found that the increase in tensile strength was largest for networks having the shortest chains (M_n = 220).

These results suggest that blending different molecular weights of the PIB telechelic ionomers might improve the tensile properties. In order to investigate this possibility, two different blends of T-8.3-Ca-0 and T-34-Ca-0 were prepared: (1) 10 mol% T-34-Ca-0 and 90 mol% T-8.3-Ca-0 and (2) 60 mol% T-34-Ca-0 and 40 mol% T-8.3-Ca-0. *Figure 20* compares the stress–strain behaviour of the two blends and the pure materials. As already discussed, T-8.3-Ca-0 has limited extension at break (~100%), and the addition of 10 mol% T-34-Ca-0 increases it to about 160%. For pure T-34-Ca-0 the tensile strength is 4.2 MPa and elongations reach 1100%. Even after adding 40 mol% T-8.3-Ca-0 the tensile properties are comparable, with a tensile strength of 4.1 MPa and elongations over 1000%. Moreover, the modulus is somewhat higher than for pure T-34-Ca-0. As *Figure 21* illustrates, the modulus can be controlled to a limited extent. Blending materials of different molecular weight therefore affords some additional control over properties, but a greater range of molecular weights would be necessary to substantiate this hypothesis fully.

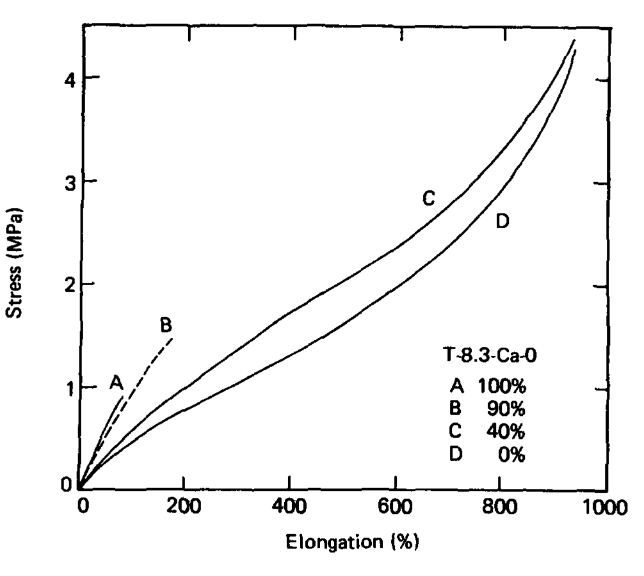

Figure 20 Effect of blend composition on the stress–strain behaviour of the T-8.3-Ca-0/T-34-Ca-0 system

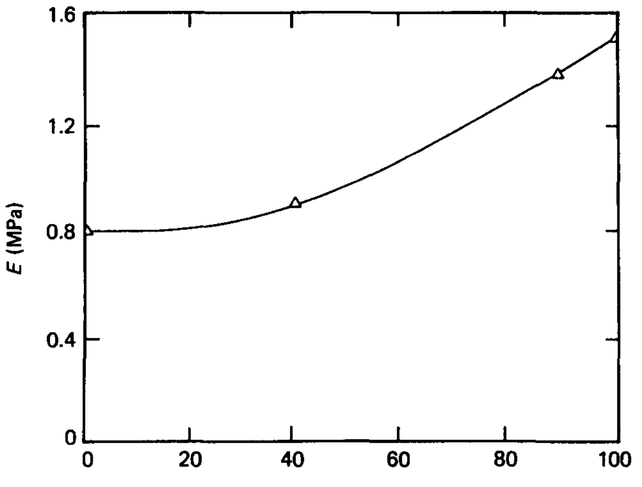

Figure 21 Effect of blend composition on the Young's modulus of the T-8.3-Ca-0/T-34-Ca-0 system

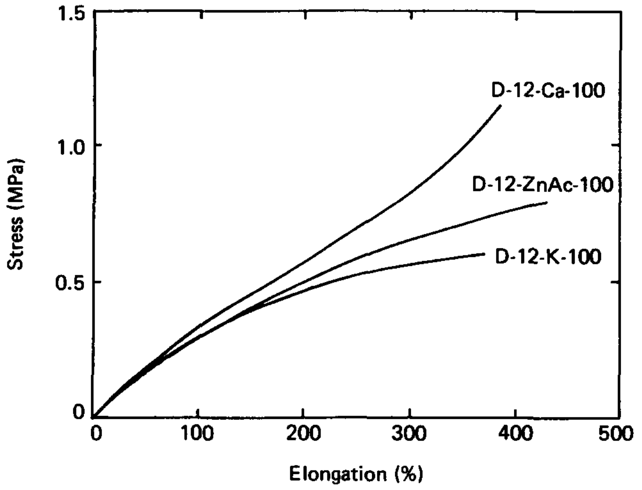

Figure 22 Effect of cation type on the stress–strain behaviour of the D-12-X-100 series

Mechanical behaviour of linear difunctional species

The linear difunctional ionomers display stress–strain behaviour which is very different from that displayed by the three-arm star trifunctional ionomers. Stress–strain curves for D-12-K-100, D-12-Ca-100 and D-12-Zn-100 are shown in *Figure 22*. Clearly, the stresses, Young's modulus and ultimate elongation ($\sim 400\%$) are all lower for the difunctional species. The effective M_c as estimated from Young's modulus is about 19 000. Recall that a similar calculation of effective M_c for the trifunctional materials yielded values of 5800–8700, depending upon the molecular weight. These results suggest that there are fewer network junction points in the difunctional materials, as would be expected. Each of the trifunctional molecules possesses a permanent network junction point while the difunctional molecules do not. *Figure 23* shows the stress–strain behaviour for D-6.5-K-100, D-6.5-Ca-100 and D-6.5-Zn-100. The ultimate elongation of these materials is only about 300%. The effective M_c for this series, calculated from Young's modulus, is only about 10 500. The effective M_c value for the 6500 $\bar{M}_n$ series is lower than that for the 12 000 $\bar{M}_n$ series because of the lower molecular weight between crosslinks and the resulting higher concentration of ionic crosslinks. The stress at any given extension is also higher for the lower-molecular-weight material as was found for the trifunctional materials.

The stress-relaxation curve for the D-6.5-K-0 material is shown in *Figure 24* for about 24 h of relaxation. Clearly, a plateau stress is not reached for this material after 1 h of relaxation as for the three-arm star trifunctional materials. This suggests that the network formed by the difunctional material is not as extensive as that formed by the trifunctional material, as would be expected. Again, the trifunctional molecules each contain a permanent trifunctional network junction point while the difunctional molecules must rely completely upon the formation of triplet or higher-order ionic associations to form a network.

The instantaneous set and hysteresis behaviour of D-6.5-K-0 are shown in *Figures 25* and *26*, respectively. The instantaneous set behaviour is seen to be comparable to that for the trifunctional materials until fracture occurs during the 350% strain cycle. The values of per cent hysteresis seem to be quite low considering the fact that the molecular weight is very low and there are no covalent trifunctional junction points.

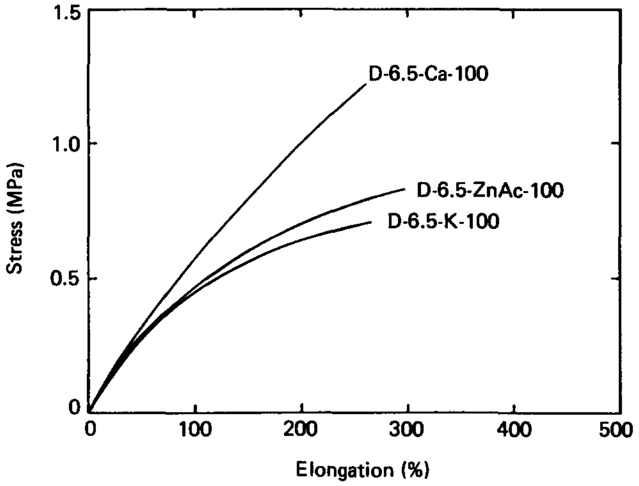

Figure 23 Effect of cation type on the stress–strain behaviour of the D-6.5-X-100 series

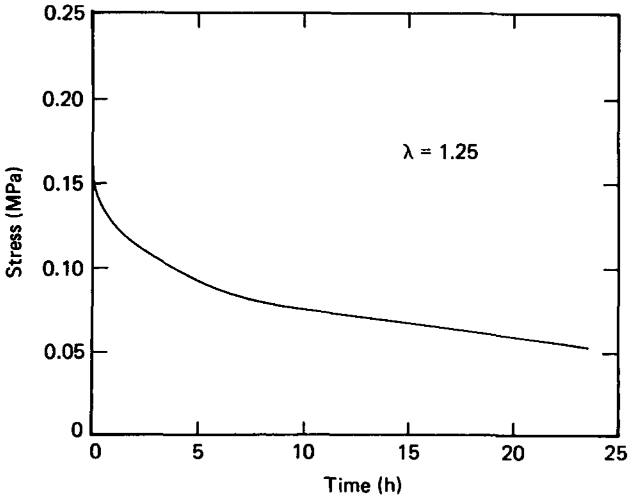

Figure 24 Stress relaxation of D-6.5-K-0

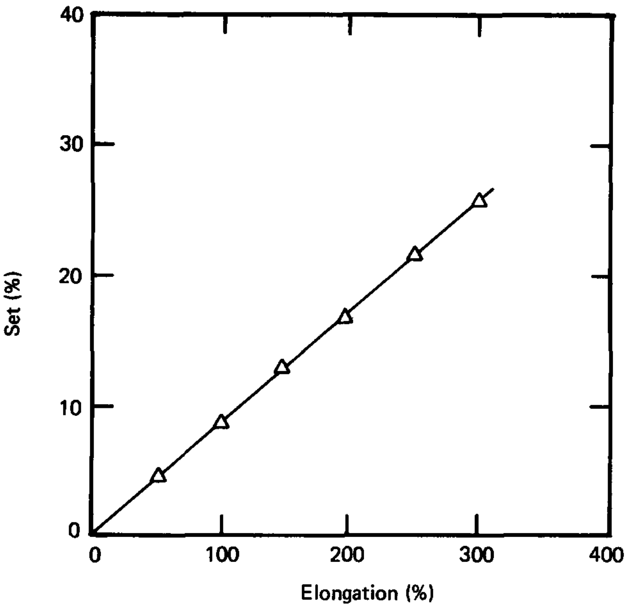

Figure 25 Instantaneous set vs. elongation for D-6.5-K-0

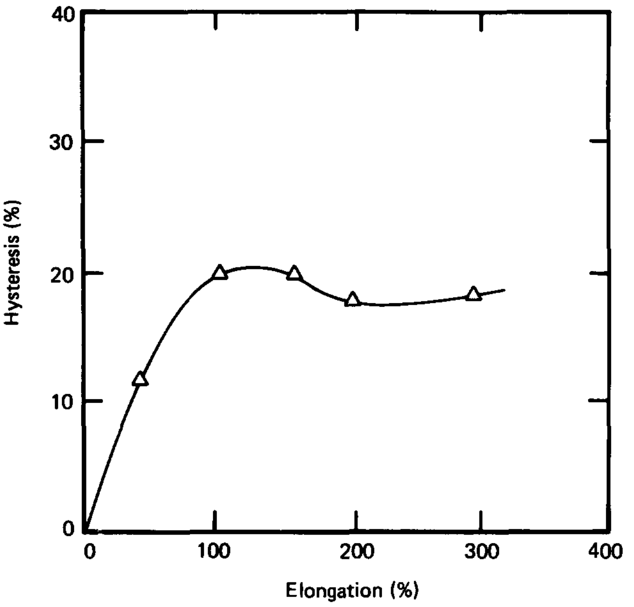

Figure 26 Mechanical hysteresis behaviour of D-6.5-K-0

Mechanical behaviour of blends of trifunctional and monofunctional species

All of the discussion thus far has concerned the three-arm star trifunctional and linear difunctional materials. The bulk properties of the linear monofunctional species could not be studied extensively due to their very poor mechanical properties. However, they do serve nicely as a model species for introducing dangling ends. Since dangling ends represent imperfections in a network structure, their presence is expected to have a detrimental effect on Young's modulus as well as on the ultimate properties. However, because of the problems of characterizing the number of dangling ends, as well as their molecular weight and distribution, very little work has been done to define quantitatively their effects on elastomeric properties. In spite of this, some useful information has been obtained concerning the effects of dangling ends on (1) the equilibrium compression modulus and degree of swelling[99,100], (2) the ultimate elongation and strength in continuous extension[100,101], (3) the viscoelastic properties in free and forced oscillations[102], and (4) the fatigue lifetime under alternating stress amplitudes[97]. Llorente *et al.*[98] investigated the dependence of ultimate properties on dangling chain irregularities in model networks of end-linked polydimethylsiloxane. It was concluded that the most important effect of dangling chain irregularities is to decrease both the maximum extensibility of a network and its ultimate strength.

Because of the model nature of the PIB telechelic ionomers, it is possible to mix the monofunctional species with the trifunctional species to study the effect of dangling ends on the mechanical properties. As an indication of the effect of the monofunctional species, the stress–strain behaviour for (1) 100% T-10.5-K-0, (2) a blend of 10% M-11-K-0 and 90% T-10.5-K-0, and (3) a blend of 22% M-11-K-0 and 78% T-10.5-K-0 is shown in *Figure 27*. The modulus was calculated from the initial slope. It was found that the Young's modulus is considerably lowered by the incorporation of the monofunctional species, from 1.1 MPa for the 100% T-10.5-K-0 to 0.76 MPa for the 10% blend and to 0.61 MPa for the 22% blend. Likewise, the ultimate elongation and tensile strength are decreased by the introduction of dangling ends. The effect upon long-term permanent set is also significant and is shown in *Figure 28*. Following elongation to an extension ratio of 7, the 24 h permanent set for T-10.5-K-0 was only 11%, while for the 10% blend it was 60% and for the 22% blend it was more than 100%. Thus the dangling ends are severely detrimental to the elastomeric properties of these materials. Interestingly, the mechanical hysteresis behaviour of the monofunctional/trifunctional blends is quite similar in terms of per cent hysteresis as a function of elongation. However, when one compares the cyclic stress–strain curves to that of the pure trifunctional material, as shown in *Figure 29*, the stresses are lower for the blends. *Figure 30* shows the stress-relaxation behaviour of these systems at an extension ratio of 1.25. From the apparent equilibrium stress values, the effective molecular weights between crosslinks, M_c, are calculated to be 8600, 13 800 and 20 000 for the pure material, the 10% blend and the 22%

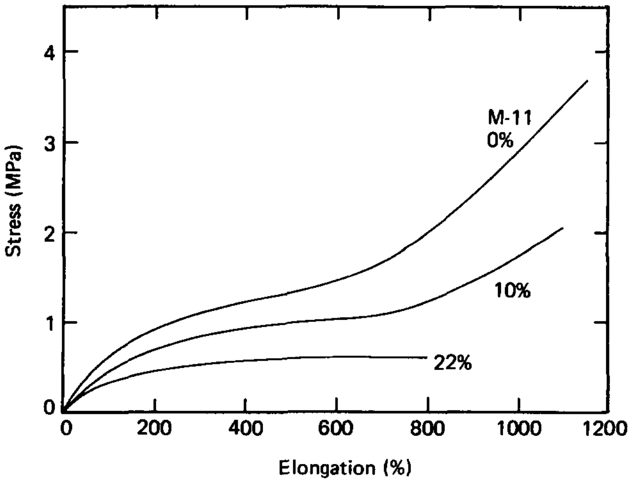

Figure 27 Effect of blend composition on the stress–strain behaviour of the T-10.5-K-0/M-11-K-0 system

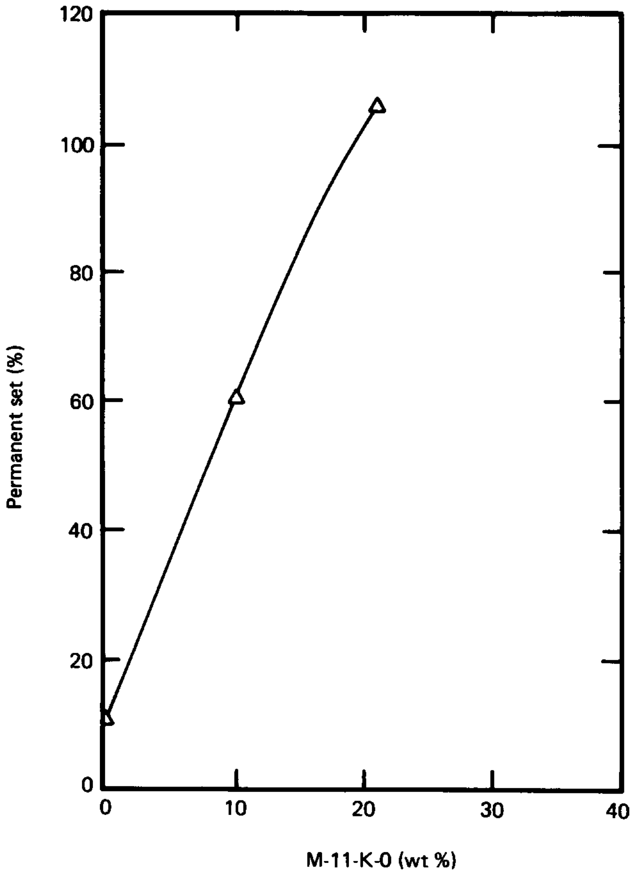

Figure 28 Effect of blend composition on the instantaneous set behaviour of the T-10.5-K-0/M-11-K-0 system

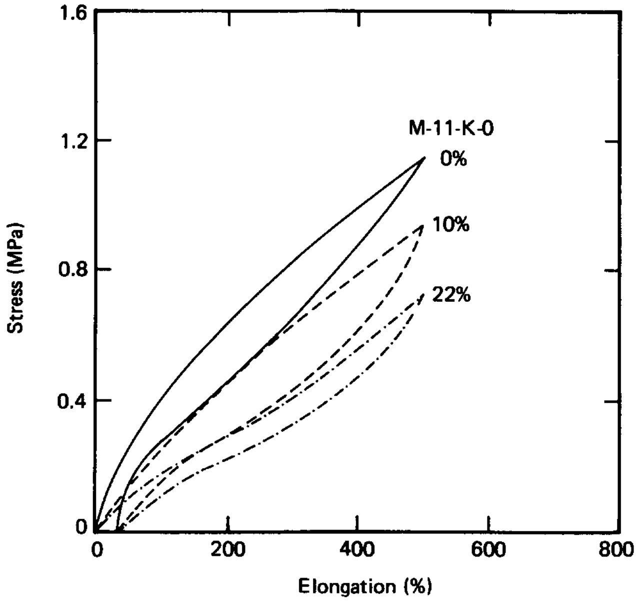

Figure 29 Effect of blend composition on the cyclic stress–strain behaviour of the T-10.5-K-0/M-11-K-0 systems

blend, respectively. It can therefore be concluded that these network defects have pronounced effects on properties, as was expected.

Several researchers have theoretically predicted the effect of dangling ends on the structure of networks[96,103–105]. In particular, Dusek and coworkers[104–106] have predicted the effect of dangling ends on their concentration of *elastic active network chains* (EANC) in a blend of monofunctional and three-arm star molecules in which it is assumed that the molecules are crosslinked at the chain ends only. According to this theory in the post-gel region, the concentration of EANC per unit volume, ν_e, is given by:

$$\nu_e = \frac{N_e d}{n_1 M_1 + n_3 M_3} \tag{4}$$

where N_e = number of EANC per primary molecule, n_1 = mole fraction of monofunctional molecules, n_3 = mole fraction of three-arm star molecules, M_1 = molecular weight of monofunctional molecules, M_3 = molecular weight of three-arm star molecules and d = density of the material. The value of N_e is given by:

$$N_e = \left(\frac{2\phi_3 - 1}{\phi_3}\right)^3 \left(\frac{\phi_3}{3 - 2\phi_3}\right) \tag{5}$$

where ϕ_3 is the mole fraction of ionic units in the three-arm star species or:

$$\phi_3 = \frac{3n_3}{3n_3 + n_1} \tag{6}$$

Using the concept of the probability generating function, Dusek and coworkers have proposed equation (4) for theoretically calculating ν_e. Experimentally, ν_e was determined from stress-relaxation data for T-10.5-K-0 and the two blends using the Gaussian theory of rubber elasticity as before. *Figure 31* shows the theoretical and experimental values of the concentration of EANCs as a function of the weight per cent of monofunctional species. For the blend systems, the experimental values are somewhat lower than those predicted from theory, but they seem to be in reasonably good agreement. The lower values may be due to some additional imperfections in the networks besides dangling ends. For example, it is possible for two chain ends of the same molecule to associate and thus act like a 'dead' cyclic or loop structure. Furthermore, experimental values may also be influenced by the molecular-weight distribution as well as possible time effects due to ion hopping.

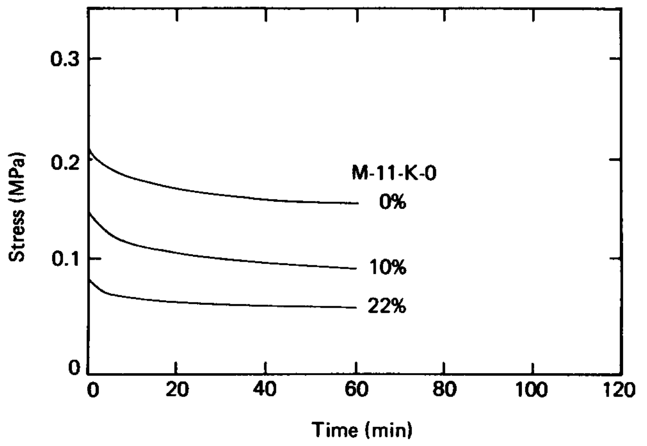

Figure 30 Effect of blend composition on the stress-relaxation behaviour of the T-10.5-K-0/M-11-K-0 series

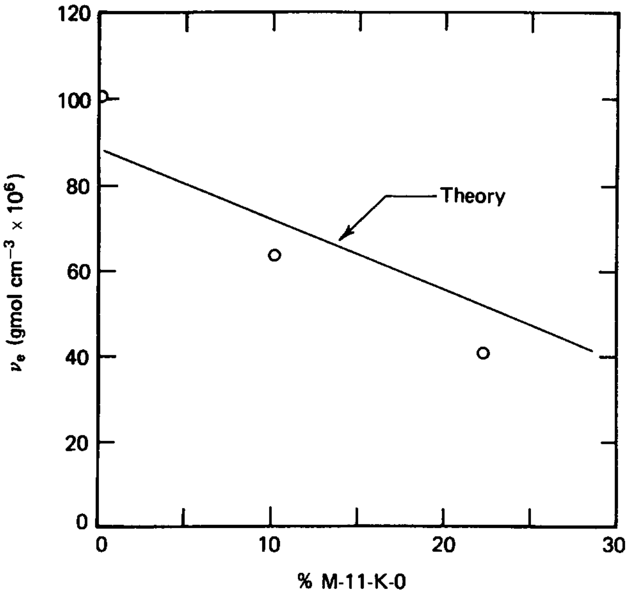

Figure 31 Effect of blend composition on the concentration, ν_e, of elastic active network chains (EANC) for the T-10.5-K-0/M-11-K-0 system

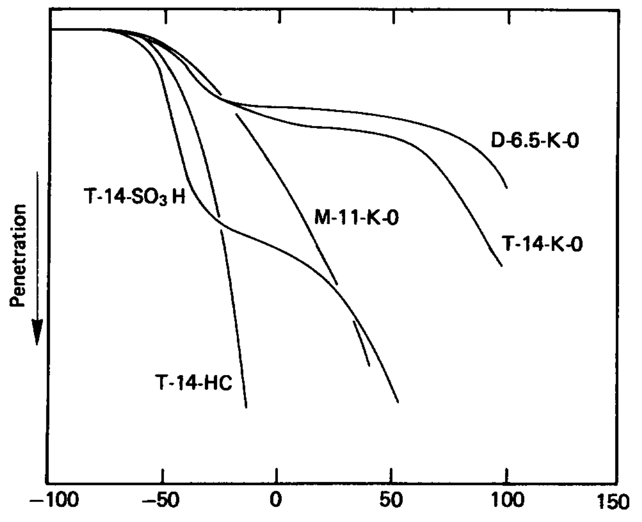

Figure 32 Effects of sulphonation, neutralization and molecular architecture on the thermomechanical behaviour of the sulphonated polyisobutylene telechelic ionomers

Thermomechanical behaviour

In order to study further the effects of ionic groups and molecular architecture, t.m.a. experiments were performed. Scans of T-14-HC, T-14-SO$_3$H, M-11-K-0, D-6.5-K-0 and T-14-K-0 are shown in *Figure 32*. All experiments were conducted at a heating rate of 10°C min^{-1}. The precursor hydrocarbon polymer (T-14-HC) flows readily above its T_g with no signs of significant intermolecular attraction. Upon sulphonation (T-14-SO$_3$) a slight rubbery plateau is observed due to the interactions of the sulphonic acid groups. Upon neutralization of the acid groups, the resulting ionomer (T-14-K-0) shows a dramatic change in its t.m.a. behaviour. Specifically, a strong rubbery plateau is observed which persists up to about 65°C. This implies that strong ionic associations occur in the neutralized ionomers. On the other hand, for the neutralized monofunctional species (M-11-K-0), no rubbery plateau is observed. This result is expected since it is not possible for the monofunctional species to form a network. Only a micellar type of structure is possible. The t.m.a. scan for the D-6.5-K-0 material shows the development of a well defined rubbery plateau region. It is therefore clear that in the difunctional materials either an ionic network is formed (requiring some triplet or higher-order associations) or extensive chain extension occurs resulting in chain entanglements. However, it is not possible to determine from these results which mechanism is dominant. It is expected that both occur to a significant degree.

From the t.m.a. studies we have seen that the rubbery plateau region for the trifunctional species extends to relatively high temperatures. However, the ionic associations are not permanent and their strength is strongly dependent upon temperature. There are two opposing forces acting on the ionic crosslinks. First, the forces arising from the entropically driven molecular motions tend to pull the chains away from the ionic aggregates. The opposing force is the coulombic force of attraction between oppositely charged ions. These forces lead to ionic crosslinking of different molecules unless intramolecular cyclization occurs. However, these coulombic forces of attraction are a weak function of temperature and tend to decrease in strength with increasing temperature. In fact, the coulombic forces are generally taken to be proportional to $\exp[z^2(r\varepsilon kT)]$, where z is the ionic charge, r is the distance between ions, ε is the dielectric constant of the medium, k is the Boltzmann constant and T is the absolute temperature[107]. Thus, above a certain temperature these ionic crosslinks can be sufficiently weakened to allow flow to occur. Since we have extensively studied and reported the melt rheological behaviour of these ionomers at temperatures well above ambient[74,75], these discussions will not be reported here. However, high-temperature stress-relaxation characteristics of some of the ionomers are presented here. *Figure 33* shows the relaxation modulus at 95°C as a function of time for the T-19-K-0, T-19-Ca-0, T-19-K-100, T-19-Ca-100, T-19-Zn-100 and T-19-CaAc-100 materials. It is seen that the materials neutralized to the equivalence point, T-19-K-0 and T-19-Ca-0, show a faster drop in modulus with time. It is noteworthy that the

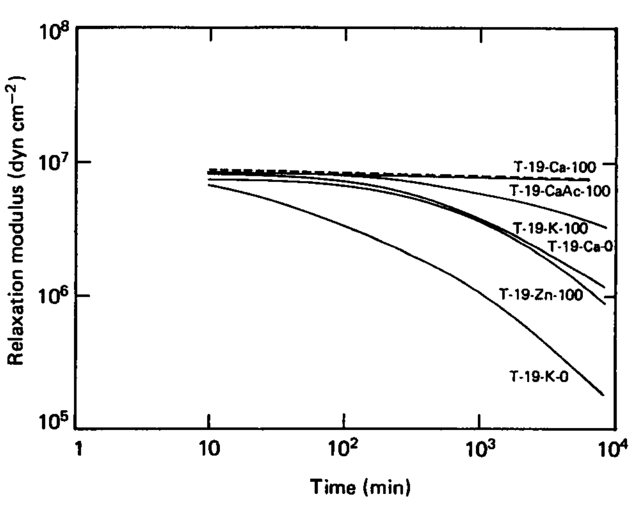

Figure 33 Stress-relaxation behaviour of the T-19 materials at 95°C

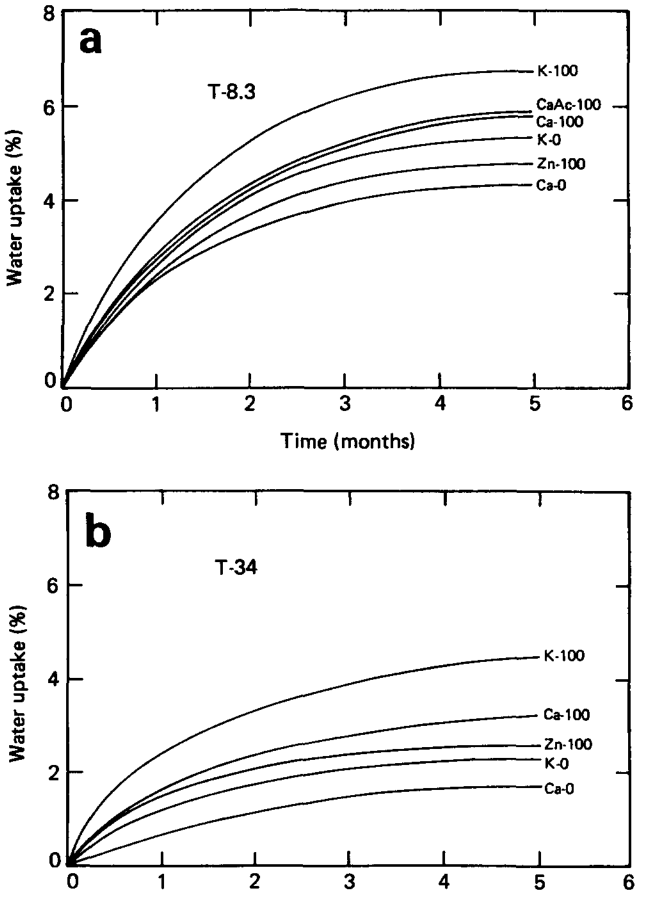

Figure 34 Water uptake as a function of time for the (a) T-8.3 and (b) T-34 series

material neutralized with monovalent potassium relaxes faster than the corresponding material neutralized with divalent calcium. As stated earlier, the ionic potential of calcium is higher than that of potassium, and hence the material neutralized with calcium relaxes more slowly. However, upon the addition of excess neutralizing agent the calcium-neutralized materials do not relax within the timescale of the experiment (about 3 h) even at 95°C, and the T-19-K-100 material relaxes much more slowly than does T-19-K-0. This is a direct consequence of increased combined coulombic attractive forces created by the presence of excess salt as discussed earlier. Another feature noted earlier is that the zinc-neutralized ionomer, T-19-Zn-100, relaxes much faster than all of the materials except T-19-K-0. Again, it is believed that this is due to the move covalent character of zinc[95].

Effect of moisture

Ionomers are generally susceptible to water absorption because of the presence of ionic groups which tend to attract more polar species such as water. For example, metal-sulphonated EPDM with only 1% ionic content absorbs up to several per cent water by weight[38]. The properties of an ionomer may also be affected by the presence of water associated with the ionic aggregates. Because of this, the effect of moisture on the stress–strain behaviour and the kinetics of water absorption in the PIB ionomers were investigated.

Strips of the ionomers were cut and immersed in distilled water. These samples were weighed from time to time over a period of *five months*. The two extreme molecular-weight materials of the trifunctional architecture, T-8.3 and T-34, were selected. *Figure 34* shows the percentage of water uptake as a function of time for the T-8.3 and T.34 series. For the T-8.3 series 4.5–6% water absorption (by weight) occurs, while the T-34 series absorbs only 1.5–3.5%. The higher water absorption in the T-8.3 series is believed to be due to the higher ionic content. The T-8.3 material contains about 2.2 mol% ions while the T-34 material contains only 0.5 mol%. It is also observed that the ionomers containing excess neutralizing agent absorb more water than the corresponding materials containing no excess salt. The zinc-neutralized ionomers generally absorb less moisture than the potassium- or calcium-neutralized materials. Similar observations were made by Lundberg and coworkers[38] for the sulphonated EPDM materials.

In another experiment, a sample of T-34-K-100 was soaked in distilled water for a few months (called the *wet* sample) and another sample of the T-34-K-0 was used directly from the vacuum desiccator (called the *dry* sample). Their stress–strain behaviour is shown in *Figure 35*. The Young's modulus remains essentially unchanged, but the ultimate strength of the wet sample is only marginally lowered. In the wet sample the water molecules may plasticize the ionic aggregates to some extent, thus weakening the strength of the aggregates.

Effect of ionic plasticizer

Makowski and Lundberg[108] have studied the effect of zinc stearate on the mechanical and rheological behaviour of EPDM-based ionomers. Zinc stearate acts as a selective ionic plasticizer in these materials, reducing the melt viscosity at elevated temperatures. However, when the material is cooled the zinc stearate crystallizes and acts as a reinforcing filler, thus enhancing the mechanical properties. Rheological studies on these PIB ionomers show a similar trend for zinc-neutralized materials[75]. It was therefore of interest to determine the effect of zinc stearate on the mechanical properties of these PIB ionomers.

A sample of T-19-Zn-100 containing 15% by weight of zinc stearate was prepared. Specifically, a known weight of T-19-Zn-100 was dissolved in a mixture of hexane and

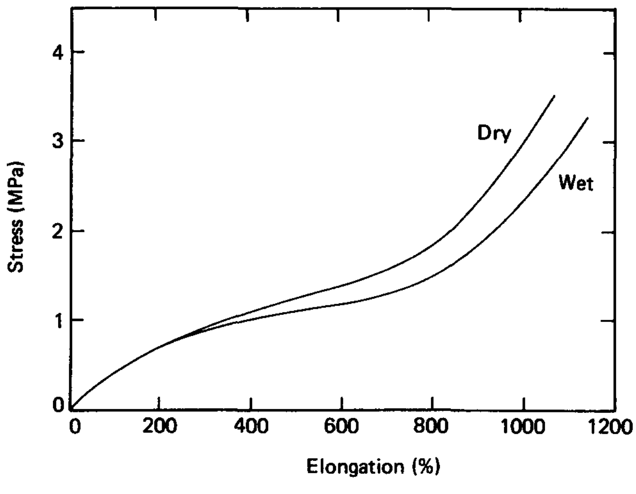

Figure 35 Effect of sorbed water on the stress–strain behaviour of T-34-K-100

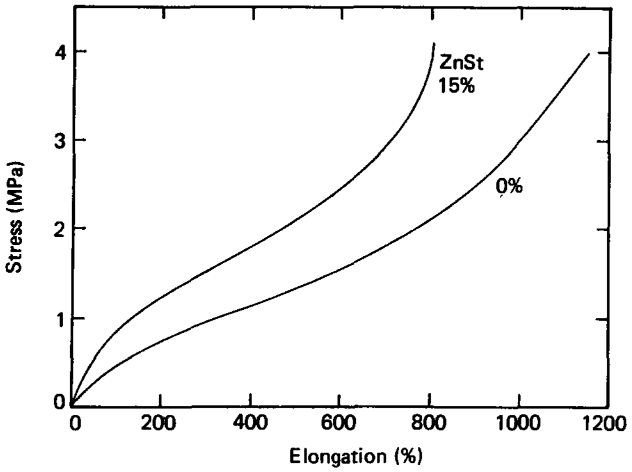

Figure 36 Effect of zinc stearate on the stress–strain behaviour of T-19-Zn-100

ethanol (95% hexane by volume) and solid zinc stearate was added to this solution. The zinc stearate did not dissolve, but appeared to remain as a finely dispersed phase. A film was cast from this solution/dispersion on a Teflon surface and dried in a vacuum oven at 70°C for 48 h. It was cut into very small pieces and compression moulded at 140°C, which is above the melting point of the zinc stearate. The film appeared to be very uniform, therefore suggesting (but not confirming) a homogeneous distribution of the zinc stearate.

A comparison of the stress–strain behaviour of T-19-Zn-100 and the same material containing 15% zinc stearate is shown in *Figure 36*. It is observed that there is a significant enhancement of the modulus and the stresses due to the zinc stearate. This is attributed to the reinforcing filler effect of the crystalline zinc stearate. The crystalline form of the zinc stearate was confirmed by WAXS. Thus with the improvement in mechanical properties at ambient temperature and the reduced viscosity at higher temperatures, zinc-neutralized PIB ionomers containing zinc stearate are probably good candidates for thermoplastic elastomers.

CONCLUSIONS

Due to the telechelic nature of these ionomers, they serve as model structures for the study of ionic interactions and the variables that influence these interactions. The addition of only two or three ionic groups per molecule changes the mechanical response from that of a viscous fluid to an elastomeric solid. The three-arm star trifunctional materials appear to form an end-linked network with an *average* of two ion pairs in each multiplet. These materials reach stresses of up to 7 MPa and elongations of up to 1000%. The linear difunctional materials reach stresses of only about 1.2 MPa and elongations of 300–400%. The linear monofunctional ionomers cannot be handled as solid materials, but can be used to study the effects of dangling chain ends in the trifunctional materials. The deformation properties (stress and strain) of the trifunctional materials are significantly reduced by blending with the monofunctional species. All of the materials flow at temperatures in the region of 160–180°C, and thus may function as thermoplastic elastomers. The trifunctional species, because of their superior mechanical properties, appear to be the best candidates for utilization as thermoplastic elastomers.

For materials above about 10000 $\bar{M}_n$, there appears to be no cluster formation due to the absence of a small-angle X-ray scattering peak. This conclusion is supported by mechanical property data which suggest that typical multiplets contain only two ionic groups. Materials below about 10000 $\bar{M}_n$ display a small-angle X-ray scattering peak, which suggests the existence of clusters, probably promoted by the high ionic content. The occurrence of strain-induced crystallization in the trifunctional ionomers at high elongations has been verified by wide-angle X-ray diffraction.

The amount of neutralizing agent present has a significant effect upon the mechanical properties of these materials. Excess neutralizing agent improves mechanical properties, but also extends the rubbery plateau to higher temperatures. This increases the required processing temperature. It is suggested that the excess neutralizing agent preferentially locates at the ionic sites and reinforces the ionic associations.

Zinc-neutralized ionomers have mechanical properties which are comparable to those of ionomers neutralized with potassium or calcium, yet they flow at lower temperatures. These materials could thus be processed at lower temperatures, thus decreasing the energy requirement. It is believed that this lower flow temperature is due to the more covalent character of zinc bonds.

These ionomers absorb very little water due to the hydrophobic nature of polyisobutylene and the low ionic content. Zinc-neutralized ionomers absorb less water than the materials neutralized with potassium or calcium.

Addition of zinc stearate enhances the mechanical properties due to a crystalline filler effect. At processing temperatures the crystals melt and the zinc stearate solvates the ionic groups to a degree. This reduces the melt viscosity and facilitates processing.

Based upon the results of this study, it is concluded that the optimum material for application as a thermoplastic elastomer might be the three-arm star trifunctional ionomer in the range 10000–20000 $\bar{M}_n$. Neutralization with zinc acetate and addition of zinc stearate would yield a material with good mechanical properties yet low viscosity at processing temperatures.

ACKNOWLEDGEMENTS

The authors gratefully acknowledge financial support for this work from the Petroleum Research Fund of the American Chemical Society (SB, MRT and GLW), the Army Research Office (SB, MRT and GLW), and the National Science Foundation (JPK).

REFERENCES

1 MacKnight, W. J. and Earnest, T. R. *J. Polym. Sci. Macromol. Rev.* 1981, **16**, 41
2 Banzuin, C. G. and Eisenberg, A. *Ind. Eng. Chem. Prod. Res. Dev.* 1981, **20**, 271
3 Longworth, R. in 'Developments in Ionic Polymers—1' (Eds. A. D. Wilson and H. J. Prosser), Applied Science, Barking, 1984
4 Mauritz, K. A. and Hopfinger, A. J. in 'Modern Aspects of Electrochemistry', No. 14 (Eds. J. O'M. Bockris, B. E. Conway and R. E. White), Plenum, New York, 1982
5 Eisenberg, A. *Macromolecules* 1970, **3**, 2
6 Eisenberg, A. and Navratil, M. *J. Polym. Sci., Polym. Lett. Edn.* 1972, **10**, 537

7 Eisenberg, A. and Navratil, M. *Macromolecules* 1973, **6**, 604
8 Navratil, M. and Eisenberg, A. *Macromolecules* 1974, **7**, 84
9 Eisenberg, A. and Navratil, M. *Macromolecules* 1974, **7**, 90
10 Weiss, R. A. and Lefelar, J. A. *Polymer* 1986, **27**, 3
11 Longworth, R. and Vaughan, D. J. *Polym. Prepr.* 1968, **9**, 525
12 Marx, C. L., Caulfield, D. F. and Cooper, S. L. *Macromolecules* 1973, **6**, 344
13 Binsbergen, F. L. and Kroon, G. F. *Macromolecules* 1973, **6**, 145
14 MacKnight, W. J., Taggart, W. P. and Stein, R. S. *J. Polym. Sci., Polym. Symp.* 1974, **45**, 113
15 Graiver, D., Litt, M. and Baer, E. *J. Polym. Sci., Polym. Chem. Edn.* 1979, **17**, 3573
16 Yarusso, D. J. and Cooper, S. L. *Macromolecules* 1983, **16**, 1871
17 Yarusso, D. J. and Cooper, S. L. *Polymer* 1985, **26**, 371
18 Jerome, R., Vlaic, G. and Williams, C. E. *J. Physique Lett.* 1983, **44**, L-717
19 Ding, Y. S., Yarusso, D. J., Pan, H. K. D. and Cooper, S. L. *J. Appl. Phys.* 1984, **56**, 2396
20 Pan, H. K., Knapp, G. S. and Cooper, S. L. *Colloid Polym. Sci.* 1984, **262**, 734
21 Pan, H. K., Maegher, A., Pineri, M., Knapp, G. S. and Cooper, S. L. *J. Chem. Phys.* 1982, **20**, 1069
22 Painter, P. C., Brozoski, B. A. and Coleman, M. M. *J. Polym. Sci., Polym. Phys. Edn.* 1982, **20**, 1069
23 Toriumi, H., Weiss, R. A. and Frank, H. A. *Macromolecules* 1984, **17**, 2104
24 Forsman, W. C. *Macromolecules* 1982, **15**, 1032
25 Forsman, W. C., MacKnight, W. J. and Higgins, J. S. *Macromolecules* 1984, **17**, 2217
26 Dreyfus, B. *Macromolecules* 1985, **18**, 284
27 Dreyfus, B. in 'Coulombic Interactions in Macromolecular Systems' ACS Symp. Ser. 302, (Eds. A. Eisenberg and F. E. Bailey), 1986
28 Brown, H. P. *Rubber Chem. Technol.* 1957, **30**, 1347
29 Brown, H. P. US Patent 2 626 248, 20th Jan. 1953
30 Brown, H. P. *Rubber Chem. Technol.* 1963, **36**, 931
31 Jenkins, D. K. and Duck, E. W. in 'Ionic Polymers' (Ed. L. Holliday), Halstead Press, New York, 1975
32 Lundberg, R. D. and Makowski, H. S. in 'Ions in Polymers', Adv. Chem. Ser. 187 (Ed. A. Eisenberg), 1980, Ch. 2
33 Canter, N. H. US Patent 3 642 728, 1974
34 Farrel, C. P. O. and Sernick, G. E. US Patent 3 836 511, 1974
35 Makowski, H. S., Lundberg, R. D. and Singhal, G. S. US Patent 3 870 841, 1975
36 Makowski, H. S., Lundberg, R. D. and Westerman, L. *Polym. Prepr.* 1978, **19**(2), 310
37 Lundberg, R. D. and Makowski, H. S. *Polym. Prepr.* 1978, **19**(2), 287
38 Makowski, H. S., Lundberg, R. D., Westerman, L. and Bock, J. in 'Ions in Polymers', Adv. Chem. Ser. 187 (Ed. A. Eisenberg), 1980, Ch. 1
39 Agarwal, P. K., Makowski, H. S. and Lundberg, R. D. *Macromolecules* 1980, **13**, 1679
40 Agarwal, P. K. and Lundberg, R. D. *Macromolecules* 1984, **17**, 1918
41 Agarwal, P. K. and Lundberg, R. D. *Macromolecules* 1984, **17**, 1928
42 Agarwal, P. K., Garner, R. T. and Lundberg, R. D. *Macromolecules* 1984, **17**, 2794
43 Peiffer, D. G. and Lundberg, R. D. *Polymer* 1983, **24**, 300
44 Sanui, K., Lenz, R. W. and MacKnight, W. J. *J. Polym. Sci., Polym. Phys. Edn.* 1974, **12**, 1965
45 Azuma, C. and MacKnight, W. J. *J. Polym. Sci., Polym. Chem. Edn.* 1978, **15**, 547
46 Rahrig, D., Azuma, C. and MacKnight, W. J. *J. Polym. Sci., Polym. Phys. Edn.* 1978, **16**, 59
47 Rahrig, D., MacKnight, W. J. and Lenz, R. W. *Macromolecules* 1979, **12**, 195
48 Rahrig, D. and MacKnight, W. J. in 'Ions in Polymers', Adv. Chem. Ser. 187, 1980, Ch. 6
49 Dieterich, D., Keberle, W. and Witt, H. *Angew. Chem. Int. Edn.* 1970, **9**, 40
50 Hwang, K. K. S., Yang, C. Z. and Cooper, S. L. *Polym. Eng. Sci.* 1981, **21**, 1027
51 Miller, J. A., Hwang, K. K. S. and Cooper, S. L. *J. Macromol. Sci.–Phys.* 1983, **B22**, 321
52 Hwang, K. K. S., Yang, C. Z., Miller, J. A. and Cooper, S. L. IUPAC 28th Macromol. Symp., 1982, p. 900
53 Hwang, K. K. S., Speckhard, T. A. and Cooper, S. L. *J. Macromol. Sci.–Phys.* 1984, **B23**, 153
54 Speckhard, T. A., Hwang, K. K. S., Yang, C. Z., Laupan, W. R. and Cooper, S. L. *J. Macromol. Sci.–Phys.* 1984, **B23**, 175
55 Otocka, E. P., Hellman, M. Y. and Blyler, L. L. *J. Appl. Phys.* 1969, **40**, 4221
56 Broze, G., Jérôme, R. and Teyssié, Ph. *Macromolecules* 1981, **14**, 225
57 Broze, G., Jérôme, R., Teyssié, Ph. and Marco, C. *Polym. Bull.* 1981, **4**, 241
58 Broze, G., Jérôme, R., Teyssié, Ph. and Gallot, B. *J. Polym. Sci., Polym. Lett. Edn.* 1981, **19**, 415
59 Broze, G., Jérôme, R. and Teyssié, Ph. *Macromolecules* 1982, **15**, 920
60 Broze, G., Jérôme, R. and Teyssié, Ph. *Macromolecules* 1982, **15**, 1300
61 Broze, G., Jérôme, R., Teyssié, Ph. and Marco, C. *Macromolecules* 1983, **16**, 996
62 Broze, G., Jérôme, R., Teyssié, Ph. and Marco, C. *J. Polym. Sci., Polym. Phys. Edn.* 1983, **21**, 2205
63 Broze, G., Jérôme, R., Teyssié, Ph. and Marco, C. *Macromolecules* 1983, **16**, 1771
64 Broze, G., Jérôme, R. and Teyssié, Ph. *J. Polym. Sci., Polym. Lett. Edn.* 1983, **21**, 237
65 Jérôme, R., Horrion, J., Fayt, R. and Teyssié, Ph. *Macromolecules* 1984, **17**, 2447
66 Broze, G., Jérôme, R., Teyssié, Ph. and Marco, C. *Macromolecules* 1985, **18**, 1376
67 Jérôme, R. and Broze, G. *Rubber Chem. Technol.* 1985, **58**, 223
68 Mohajer, Y., Tyagi, D., Wilkes, G. L., Storey, R. F. and Kennedy, J. P. *Polym. Bull.* 1982, **8**, 47
69 Bagrodia, S., Mohajer, Y., Wilkes, G. L., Storey, R. F. and Kennedy, J. P. *Polym. Bull.* 1982, **8**, 281
70 Bagrodia, S., Mohajer, Y., Wilkes, G. L., Storey, R. F. and Kennedy, J. P. *Polym. Bull.* 1983, **9**, 174
71 Mohajer, Y., Bagrodia, S., Wilkes, G. L., Storey, R. F. and Kennedy, J. P. *Polym. Bull.* 1983, **9**, 174
72 Mohajer, Y., Bagrodia, S., Wilkes, G. L., Storey, R. F. and Kennedy, J. P. *J. Appl. Polym. Sci.* 1984, **29**, 1943
73 Bagrodia, S. R., Wilkes, G. L. and Kennedy, J. P. *J. Appl. Polym. Sci.* 1985, **30**, 2179
74 Bagrodia, S., Pisipati, R., Wilkes, G. L., Storey, R. F. and Kennedy, J. P. *J. Appl. Polym. Sci.* 1984, **29**, 3065
75 Bagrodia, S., Wilkes, G. L. and Kennedy, J. P. *Polym. Eng. Sci.* 1986, **26**, 62
76 Tant, M. R., Song, J. H., Wilkes, G. L. and Kennedy, J. P. *Polym. Prepr.* 1986, **27**(1), 351
77 Tant, M. R., Wilkes, G. L., Storey, R. F. and Kennedy, J. P. *Polym. Bull.* 1985, **13**, 541
78 Tant, M. R., Wilkes, G. L., Read, M. D. and Kennedy, J. P. *J. Polym. Sci., Polym. Lett. Edn.* 1986, **24**, 619
79 Tant, M. R., Song, J. H., Wilkes, G. L., Horrion, J. and Jérôme, R., *Polymer* 1986, **27**, 1815
80 Kennedy, J. P., Huang, S. Y. and Feinberg, S. C. *J. Polym. Sci., Polym. Chem. Edn.* 1977, **15**, 2869
81 Kennedy, J. P. and Smith, R. A. *J. Polym. Sci., Polym. Chem. Edn.* 1980, **18**, 1523
82 Kennedy, J. P., Ross, L. R., Lackey, J. E. and Nuyken, O. *Polym. Bull.* 1981, **4**, 67
83 Kennedy, J. P., Chang, V. S. C., Smith, R. A. and Ivan, B. *Polym. Bull.* 1979, **1**, 57
84 Kennedy, J. P. and Storey, R. F. *Org. Coat. Appl. Polym. Sci.* 1982, **46**, 182
85 Kennedy, J. P. and Storey, R. F. IUPAC 28th Macromol. Symp., 1982, p. 905
86 Storey, R. F. Ph.D. Dissertation, The University of Akron, 1983
87 Tant, M. R., Venkateshwaran, L., Huang, H., Wilkes, G. L. and Kennedy, J. P., in preparation
88 Mark, J. E. *Adv. Polym. Sci.* 1982, **44**, 1
89 Mark, J. E. *J. Chem. Educ.* 1981, **58**, 898
90 Hara, M., Eisenberg, A., Storey, R. F. and Kennedy, J. P. in 'Coulombic Interactions in Macromolecular Systems', ACS Symp. Ser. 302, (Eds. A. Eisenberg and F. E. Bailey), 1986
91 Mooney, M. *J. Appl. Phys.* 1948, **19**, 434
92 Rivlin, R. S. *Phil. Trans. R. Soc. Lond. A* 1948, **241**, 379
93 Bagrodia, S., Ph.D. Dissertation, Virginia Polytechnic Institute and State University, 1984
94 Matsuura, H. and Eisenberg, A. *J. Polym. Sci., Polym. Phys. Edn.* 1983, **21**, 595
95 Bagrodia, S. and Wilkes, G. L. *Polym. Bull.* 1984, **12**, 389
96 Andray, A. L. and Mark, J. E. *J. Appl. Polym. Sci.* 1981, **26**, 1829
97 Llorente, M. A. and Mark, J. E. *J. Chem. Phys.* 1979, **71**, 682

98 Llorente, M. A., Andray, A. L. and Mark, J. E. *J. Polym. Sci., Polym. Phys. Edn.* 1981, **19**, 621
99 Flory, P. J., Crescenzi, V. and Mark, J. E. *J. Am. Chem. Soc.* 1964, **86**, 146
100 Mark, J. E. *Polym. Eng. Sci.* 1979, **19**, 409
101 Mark, J. E. and Sullivan, J. L. *J. Chem. Phys.* 1977, **66**, 1006
102 Flory, P. J. 'Statistical Mechanics of Chain Molecules', Interscience, New York, 1969
103 Miller, D. R. and Macosko, W. *Macromolecules* 1976, **92**, 206
104 Dusek, K. *Rubber Chem. Technol.* 1982, **55**, 1
105 Dusek, K. and Prins, W. *Adv. Polym. Sci.* 1969, **6**, 1
106 Dusek, K. and Vojta, V. *Br. Polym. J.* 1977, **6**, 184
107 Fuoss, R. M. and Accascina, F. 'Electrolytic Conductance', Interscience, New York, 1959
108 Makowski, H. S. and Lundberg, R. D. in 'Ions in Polymers', Adv. Chem. Ser. 187, (Ed. A. Eisenberg), 1980, Ch. 3